

THE EFFECTS OF THERMO-MECHANICAL TREATMENTS ON
PRECIPITATE MORPHOLOGY OF AL 2036

by

Ray Doucette

A THESIS

SUBMITTED TO THE FACULTY OF GRADUATE STUDIES
IN PARTIAL FULFILMENT OF THE REQUIREMENTS FOR THE DEGREE
OF MASTER OF SCIENCE

DEPARTMENT OF MECHANICAL ENGINEERING

UNIVERSITY OF MANITOBA

WINNIPEG, MANITOBA

MAY 1977

THE EFFECTS OF THERMO-MECHANICAL TREATMENTS ON
PRECIPITATE MORPHOLOGY OF AL 2036

BY

RAY DOUCETTE

A dissertation submitted to the Faculty of Graduate Studies of
the University of Manitoba in partial fulfillment of the requirements
of the degree of

MASTER OF SCIENCE

© 1977

Permission has been granted to the LIBRARY OF THE UNIVER-
SITY OF MANITOBA to lend or sell copies of this dissertation, to
the NATIONAL LIBRARY OF CANADA to microfilm this
dissertation and to lend or sell copies of the film, and UNIVERSITY
MICROFILMS to publish an abstract of this dissertation.

The author reserves other publication rights, and neither the
dissertation nor extensive extracts from it may be printed or other-
wise reproduced without the author's written permission.

TABLE OF CONTENTS

LIST OF FIGURES	I
ACKNOWLEDGMENT	III
ABSTRACT	IV
1. INTRODUCTION AND OBJECTIVES	1.
2. LITERATURE REVIEW	2.
2.1. Effect of Prestrain and Temperature of Prestrain on Precipitation Hardening and Dislocation Substructure	2.
2.2. Thermal Mechanical Treatments of Aluminum Alloys	6.
2.3. Structure of Precipitates in Al-Cu-Mg Alloys	8.
3. EXPERIMENTAL TECHNIQUES	13.
3.1. Alloy Studied	13.
3.2. Thermal Mechanical Treatments	14.
3.2.1. Heat Treatment	14.
3.2.2. Mechanical Treatment	14.
3.2.3. Mechanical Testing	14.
3.3. Structural Examination	16.
3.3.1. Optical Microscopy	17.
3.3.2. X-ray Diffraction Techniques	17.
3.3.3. Electron Microscopy	18.
4. EXPERIMENTAL RESULTS	19.
4.1. Mechanical Properties	19.
4.2. Structure of Thermo-Mechanically Treated Specimens	22.
4.2.1. Solution Treated and Deformed Specimens	22.
4.2.2. Aged Specimens	23.

5.	DISCUSSION OF RESULTS	42.
6.	REFERENCES	51.
7.	MICROGRAPHS	53.

LIST OF FIGURES

2.1.	Formation of a Composite Precipitate Sheet of S(Al_2 Cu Mg).	10.
3.1.	The Blanks for Tensile Specimens.	15.
4.1.	Aging and Elongation Curves of Undeformed Material Aged at 100°C and Room Temperature.	29.
4.2.	Aging and Elongation Curves of Undeformed Material aged at 150°C and 190°C.	31.
4.3.	Aging and Elongation Curves of Deformed Material aged at 150°C. 10% Deformation at Room Temperature, 50°C, and 100°C.	33.
4.4.	Aging and Elongation Curves of Deformed Material Aged at 150°C. 30% Deformation at Room Temperature, 50°C, and 100°C.	35.
4.5.	Aging Curves of Material Deformed 10% and 30% at room temperature.	37.
4.6.	Aging Curves of Material Deformed 10% and 30% at 50°C.	39.
4.7.	Aging Curves of Material Deformed 10% and 30% at 100°C.	41.
5.1.	The σ_y Max. at 150° Aging vs. Percent Deformation at Various Temperature	42b.
7.1A.	Structure of the alloy 10% deformed at room temperature. The hexagonal particles undissolved in solution treatment are shown.	55.
7.1B.	Structure of material solution treated and aged 3200 hours at room temperature	55.
7.2.	Cellular structure of material 30% deformed at room temperature	57.
7.3.	Cellular structure of material 10% deformed at room temperature	57.
7.4.	Structure of material 30% deformed at 100°C.	59.
7.5	Structure of material 10% deformed at 100°C.	59.

7.6.	Structure of specimen aged 70 hours at 150°C.	61.
7.7.	Structure of a specimen aged 170 hours at 150°C. [(001) foil normal]	61
7.8.	Structure of a specimen aged 170 hours at 150°C. [(011) foil normal]	63.
7.9	Selected area diffraction pattern of Figure 7.7	63.
7.10.	Structure of a specimen aged 500 hours at 150°C.	65.
7.11A.	Structure of material aged 165 hours at 300°C.	65.
7.11B.	Dark field of Figure 7.11A taken with (002) diffraction spot	67.
7.12.	Diffraction pattern of Figure 7.11	67.
7.13.	Structure of material 30% deformed at 100°C and aged 1 hour at 150°C.	69.
7.14.	Structure of material 30% deformed at temperature aged 1 hour at 150°C	69.
7.15.	Structure of material 30% deformed at 100°C and aged 100 hours at 150°C.	71.
7.16.	Structure of material deformed 30% at 100°C and aged 2.5 hours at 190°C.	71.
7.17.	Dark field of Figure 7.16.	73.
7.18.	Structure of material deformed 30% at 100°C and aged 23 hours at 190°C.	73.
7.19.	Structure of material 30% deformed at 100°C and aged 188 hours at 190°C [(001) foil normal].	75.
7.20.	Dark field of Figure 7.19 from (011) precipitate diffraction spot.	75.

ACKNOWLEDGMENT

I wish to express my sincere thanks to Dr. M.C. Chaturvedi for his patient guidance and financial assistance throughout the course of this work.

The financial assistance from the Department of Mechanical Engineering is gratefully acknowledged.

I would like to thank Dr. D.J. Lloyd and Alcan who supplied the material for this project.

ABSTRACT

The effects of prestrain and the temperature of prestrain on the precipitate morphology and the dislocation structure in Al 2036 were studied. It was found that $\theta(\text{CuAl}_2)$ was the precipitate responsible for strengthening. Prestrain of the material accelerates the formation of the θ' precipitate, which is the major strengthening structure, and shortens the time required to reach maximum strengths. Raising the temperature of prestrains into the dynamic strain aging regions causes a more uniform dislocation structure rather than the cellular type of structure seen upon deformation at room temperature. The combined effect of the more rapid nucleation and more uniform dislocation structure results in an increment in strength that is retained at all stages of the aging curves.

1. INTRODUCTION AND OBJECTIVES

Thermal mechanical treatments (TMT) are the combination of strain hardening and heat treatments to introduce the substructure necessary to meet the increasing demands on materials. The advantage of TMT is that they can be incorporated into the existing fabrication and heat treatment procedures with relatively small increases in fabrication cost. Traditional means of strengthening such as alloying or extended heat treatments can be costly and time consuming. Therefore it would be advantageous to produce a finished product with TMT in the fabrication cycle to achieve the necessary properties.

During the present investigations aluminum alloy 2036, which has been developed for autobody application, was used. The TMT studied involved a variation in prestrain and the temperature of prestraining. The solution treatment, quench rate, strain rate and aging temperature were constant. The object of this study was to understand the effect of these variables on precipitation behaviour, dislocation substructure and mechanical properties of aluminum 2036 alloy.

2. LITERATURE REVIEW

In order to understand the effects of TMT it is necessary to understand the effect variable treatments will have on the properties of the material studied. As such, information on the effects of TMT and the possible structures of precipitates in Al2036 has been compiled in the following sections.

2.1. Effect of Prestrain and Temperatures of Prestrain on PPT Hardening and Substructure

It is well know that the deformation of solution treated material results in a profuse multiplication of dislocations. Also the density of dislocations increases with an increasing plastic strain. The interaction of these dislocations with each other and with obstacles such as precipitates cause the flow stress of the material to increase and therefore harden the material.

The deformation substructures are a function of one material variable, Stacking Fault Energy, and three experimental variables: the degree of plastic strain, deformation temperature, and strain rate⁽¹⁾. The SFE in a particular material must be high enough ($> .03 \text{ J/m}^2$) to allow the processes of cross slip and climb to take place relatively easily in order to compare the substructures of various materials. The degree of plastic strain and the deformation temperature

interact to produce a substructure of tangles and, or dislocation cells with cell walls of high dislocation density. It is the refinement of this substructure to produce the best mechanical properties that is of interest in thermal mechanical treatments.

Dislocation density (ρ) in deformed metals shows a definite relation with flow stress of the form

$$\sigma_f = \sigma_o + \alpha G \bar{b} \rho^{1/2} \quad (1)$$

where σ_o is the friction stress, G the shear modulus, \bar{b} the Burgers vector, and α a constant referred to as the dislocation strengthening efficiency. It has been shown⁽²⁾ in investigations of iron that the flow stress is directly related to the cell-interior dislocation density through equation (1). Therefore it is important to realize that not the production of a high average dislocation density but the production of a uniformly dispersed dislocation network is important.

The effect of prestrain on precipitation hardening has been observed by many authors. The nucleation of precipitates in a metastable matrix is dependent upon three energy changes, the volume free energy change, the strain energy change produced in the lattice by the precipitate, and the increase in interfacial energy due to the formation of the new precipitate-matrix interface. Therefore, the total change in free energy,

$$\Delta F = \Delta F_{\text{volume}} + \Delta F_{\text{surface}} + \Delta F_{\text{strain}} \quad (2)$$

A precipitate will form, if the nucleus is above critical size, when the release of volume free energy is enough to provide the surface and strain energy of the precipitate. When dislocations are present their elastic strain will accommodate the strain energy of the precipitate and the resistance to growth of the precipitate is lowered.

Wilson and Partridge⁽³⁾ working on an Al - 2.5% Cu - 1.2% Mg, laboratory prepared alloy, found that precipitate refinement by prestrain prior to aging was possible. Since the precipitates were heterogeneously nucleated at dislocations, for a given solute content, the final precipitate size would be smaller.

Pashley et al⁽⁴⁾ studying Al-Mg -Si alloys showed that the precipitates tend to nucleate preferentially on dislocation configurations and grain boundaries.

A.A. Tavassoli⁽⁵⁾ working on various Aluminum alloys found that deformation before aging would decrease the average size of both the S' and θ' precipitates. It appeared that extra dislocation introduced by deformation before aging had provided additional nucleation sites for θ' and S' and thus had refined their size.

Another effect of prestrain on precipitation hardening is that the rate of nucleation of an intermediate precipitate is increased. Silcock^(6,7) found that in Al-Cu alloys the

intermediate structure θ' forms after much shorter aging times if the alloy is cold worked between solution treatment and aging. This has a tendency to increase the maximum hardness of the alloy although the increment of hardness during aging may be less than in the unworked alloy.

The effect of the temperature of prestrain with respect to precipitate hardening and dislocation substructure can best be described in the light of dynamical strain aging of alloys⁽⁸⁾. In substitutional alloys the normal Portevin-Le Chatelier effect is generally observed only after a critical amount of strain, which increases with increasing strain rate and decreasing temperature. It has been shown⁽⁹⁾ that prestrain in the dynamic strain aging region will produce a dislocation substructure of high dislocation density with little cell formation.

Work done by J.G. Morris⁽¹⁰⁾ states that the recrystallization kinetics of dynamically strain ageable aluminum alloys are in part determined by the intensity of dynamic strain aging that occurs during the cold working of these alloys. The locking of dislocations by solute configurations produces a more stable dislocation structure. It has also been shown that all aluminum alloys in the completely solution treated condition possess a large degree of dynamic strain ageability. Morris found that Al-4% Cu with an initial solid solution condition and deformed at room temperature showed a notable degree of dynamic strain aging.

2.2. Thermal Mechanical Treatments of Al Alloys

Thermal mechanical treatments have achieved a large degree of success in many Aluminum alloys. Generally the control of precipitation hardening and modification of dislocation substructure in the alloys are the mechanisms used to improve material performance.

Burdon and Martin⁽¹¹⁾ found that room temperature yield stress could be increased in Al-1.2% Mn-0.4% Zr by the TMT of the alloy with its finely dispersed second phase. With the second phase produced by preaging the work hardening increment was much higher than without the second phase. This is thought to be due to the non-coherent dispersion of Al₃Zr causing greater dislocation multiplication. The increase in hardness persists over many cycles of aging and deformation.

H.A. Lipsitt et al⁽¹²⁾ have looked at dislocation substructures produced in aged Al-2.5% Cu, 2024, and 7075 Aluminum alloys by repeated rolling and recovery cycles. The stability of the dislocation substructures result in a retention of the strengthening after exposure at elevated temperatures. This stability is apparently due to the restriction of ledge motion by second phase particles. This statement was supported by work done by Wilson and Joffe⁽¹⁸⁾ and by Webster⁽¹⁹⁾ who say dislocation substructures developed in processing oxide dispersed materials may be responsible for $\frac{1}{4}$ to $\frac{1}{2}$ of their high temperature yield strength. One of

the suggestions was that the particles stabilized the substructure by preventing recrystallization.

In work by Tavossoli⁽⁵⁾ using many Al alloys the effect of deformation before aging was investigated. It was found that, in addition to the work-hardening effect, alloys with heterogeneous nucleation display an increase in maximum strength. The additional nucleation sites cause a refinement of the intermediate precipitates. Also the preferential nucleation of the intermediate precipitate which is responsible for the maximum hardening is at the expense of the formation of G.P. zones. Therefore there is an accelerated rate of age hardening.

It appears that two major hardening mechanisms are affected by TMT. The dislocation substructure and the precipitation of a second phase interact to form a stronger and more stable material. It would seem reasonable to assume that some maximum strengthening effect could be achieved by obtaining the greatest contribution to strength from each mechanism.

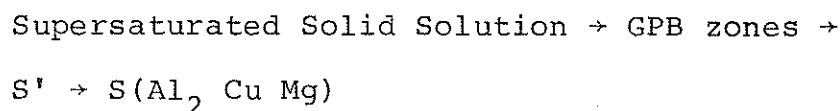
In conclusion it has been shown that the introduction of a profuse dislocation network causes refinement of the precipitated phase and accelerates the growth of an intermediate precipitate. Also it has been shown that the second phase particles have a pronounced effect on the type of dislocation network formed and the rate at which recovery and recrystallization will take place in the matrix. The deformation of a material at a temperature where dynamic

strain aging takes place will produce a uniform distribution of dislocations. By precipitation on these dislocations the substructure can be stabilized, thus, producing a maximum strengthening effect by a uniform distribution of dislocations as well as precipitates. As such, deformation at progressively higher temperatures in a dynamic strain aging temperature region should increase the mechanical properties until the recovery and recrystallization of the dislocation substructure reverses the effect of deformation.

2.3. Structure of Precipitates in Al-Cu-Mg Alloys

In Al-Cu-Mg alloys two types of precipitates can be responsible for the precipitation hardening of the alloy. Both have been well documented and the features necessary to recognize either of the two precipitates will follow.

One possibility is the ternary Al_2CuMg structure referred⁽¹³⁾ to as the S-phase which is orthorhombic with $a = 4.00$, $b = 9.23$, $c = 7.14\text{\AA}$. It appears the precipitation process can be represented by the following scheme⁽³⁾:



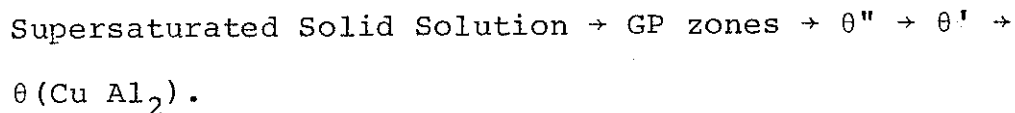
The major strengthening precipitate is the intermediate precipitate S' which has a slightly distorted S structure, but with a different matrix precipitate coherence. Silcock⁽¹⁴⁾ has shown the S structure is unlikely to transform at aging

temperatures under 450°C.

The morphology of the S' precipitate has been studied in detail by Wilson and Partridge⁽³⁾ who have shown laths of S' precipitates growing on {210} planes in the < 001 > directions. These laths laying on {210} planes form corrugated sheets of precipitate as shown in Figure 2.1. The S' precipitates were shown to have the following orientation relationship with the Aluminium matrix:

$$[100]_S // [100]_{Al}, [010]_S // [021]_{Al}, [001]_S // [012]_{Al}$$

A second possibility is the Al Cu binary system. Extensive work has been done on Al-4% Cu alloy by Thomas and Whelan⁽¹⁵⁾. The precipitation of θ , $CuAl_2$, can be represented by:



The θ structure was identified as tetragonal with $a = b = 6.066 \text{ \AA}$ and $c = 4.874 \text{ \AA}$ (Bradly and Jones 1933). Thomas and Whelan⁽¹⁵⁾ show in Al-4% Cu alloy that though the θ phase may be present at aging temperatures less than 250°C the quantity is insufficient to give appreciable diffraction. At temperatures of $\sim 330^\circ\text{C}$ the growth of θ precipitates at the expense of θ' occurs fairly rapidly.

The θ' structure has been identified as tetragonal⁽¹⁷⁾ with $a = b = 4.04 \text{ \AA}$ and $c = 5.8 \text{ \AA}$. Thomas and Nutting⁽²⁰⁾

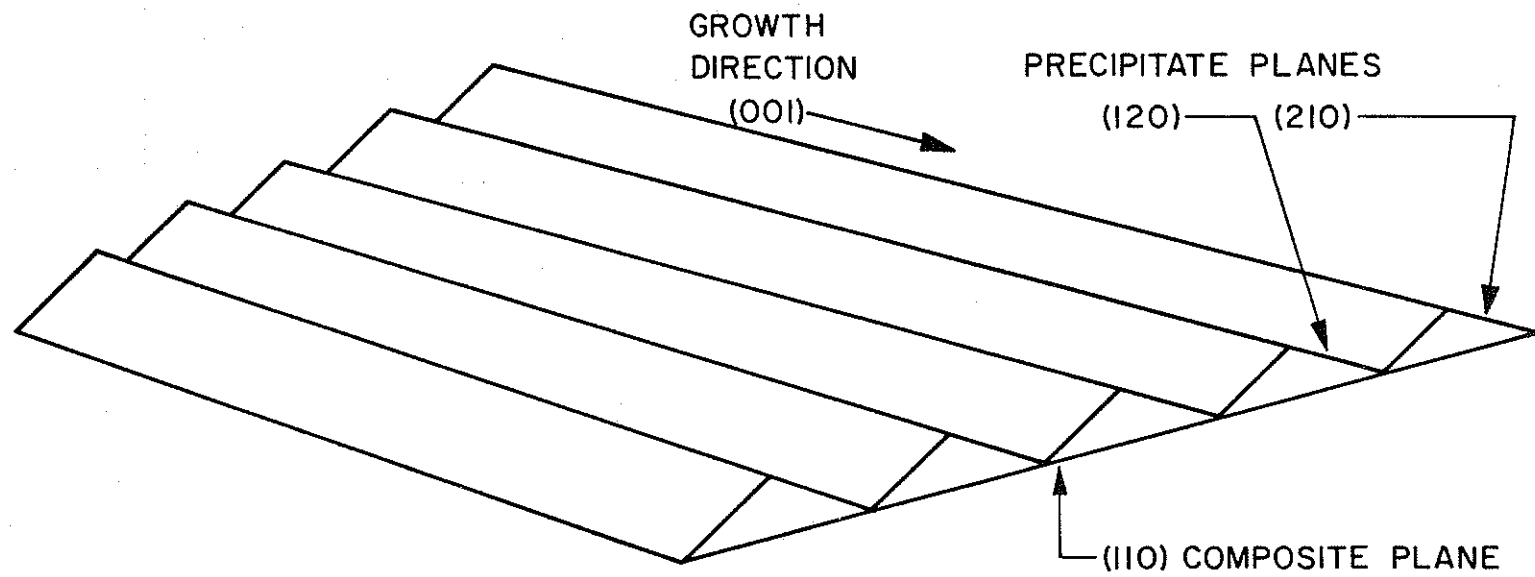


Figure 2.1 The formation of a composite precipitate sheet on a (110) plane by the growth of precipitate lath on (120) and (210) planes in the $[001]$ direction.

describe the θ' phase as definite white plates on $\{100\}$ matrix planes. The heterogeneous nucleation of θ' on dislocations accounts for an appreciable fraction of the total θ' precipitation⁽⁶⁾.

The θ'' or GP_2 structure has been identified as⁽¹⁶⁾ tetragonal with $a = b = 4.04\text{\AA}$ and c varying between 7.6 and 8.2 \AA depending on the heat treatment. The orientation relationship of θ'' as is θ' with the Aluminum matrix is as follows:

$$\{100\}_{\text{ppt}} // \{100\}_{\text{matrix}}$$

The effect of Cu:Mg ratio on the structure of the precipitate was studied by Silcock⁽¹⁴⁾. Her work looked at the aging characteristics of high purity alloys with Cu:Mg ratios of 7:1 and 2.2:1. The structure of precipitates in the alloy with a ratio of 2.2:1 followed the scheme of the $S(\text{Al}_2\text{CuMg})$ precipitates from G.P.B. only at low-temperature aging to S' and S at higher temperatures of aging. The alloys with a ratio of 7:1 showed the concurrent formation of both the S and the θ CuAl_2 structures. At the maximum strengths the S' and θ' were always the most prominent structure.

A.A. Tavassoli⁽⁵⁾ studied commercial aluminum alloys with Cu:Mg ratios of 4.5:1 and 1.92:1. The alloy with a ratio of 1.92:1 had a nominal composition of Al-2.5 Cu-1.3% Mg-1% Fe-0.08% Mn-1.0% N_1 -0.08% Zn-0.07% Ti-0.7% Si. In this

alloy the sequence of precipitation followed the $S(Al_2 Cu Mg)$ scheme. The alloy with a ratio of 4.5:1 and nominal composition of Al-4% Cu-0.89% Mg-1.0% Fe-1.2% Mn-0.2% Ni-0.2% Zn-0.90% Si showed no S type of precipitation. The precipitation sequence followed that of the $\theta(Cu Al_2)$ binary alloy.

The effect of Si on the nature of precipitation in Aluminum alloys has been studied by Wilson et al⁽²¹⁾. They concluded that Si decreases the rate of GPB formation but increases the coherency strain associated with their formation. Also a more dense and uniform distribution of S' precipitates is noticed in the silicon bearing alloy. Both of these affects will have a strengthening effect on the material.

The effect of Iron on Al-2.5% Cu-1.2% Mg alloy was studied by Wilson and Forsyth⁽²²⁾. The iron produced a coarse intermetallic primary phase that would not dissolve at solution treatment temperatures. Both, the plateau reached at room temperature hardening and the rate of hardening to this plateau were decreased. At higher temperature aging the iron had no effect on the rate of nucleation and growth of the intermediate precipitate.

The effect of MANGANESE on the aging behaviour of Al-4.2% Cu alloy was studied by Matsuo and Hiratu⁽²³⁾. They suggested that a retardation of age hardening occurred with increasing Mn, and in an alloy containing 0.5 wt% Mn no effective age hardening occurred after several weeks. It has also been proposed⁽²⁴⁾ that Mn functions as a hardener by anchoring the dislocations round the dissolved atoms.

3. EXPERIMENTAL TECHNIQUES

3.1. Alloy Studied

The alloy was received from Alcan in the form of 0.10 cm sheet. It was Reynolds aluminum alloy with the following compositional limits.

Element	Limit %
Silicon	0.5 max
Iron	0.5 max
Copper	2.2 → 3.0
Manganese	0.1 → 0.4
Magnesium	0.3 → 0.5
Chromium	0.1 max
Zinc	0.25 max
Titanium	0.15 max
Others each	0.05 max
Others total	0.15 max
Aluminium	Balance

A chemical analysis of the six major elements gave

Copper	2.39%
Magnesium	.42
Manganese	.25
Iron	.37
Silicon	.24
Aluminium	Balance

3.2. Thermal Mechanical Treatment

3.2.1. Heat Treatments

The solution treatments were carried out at 535°C for 24 hours and were quenched in water at room temperature. Each specimen was wrapped in steel foil during the heat treatment. A silicon oil bath was used for aging treatments at 100°C and 150°C. The aging at room temperature was carried out in air and the 190°C aging was achieved in a forced air furnace.

3.2.2. Mechanical Treatment

The mechanical treatment of the solution treated samples was done by rolling at a rate of 31 ft./min. in a Stanet 316 rolling mill with variable temperature rolls. When deforming the material at the various temperatures of room temperature, 50°C and 100°C the specimens were preheated to the rolling temperature in a water bath for a period of 5 minutes.

3.2.3. Mechanical Testing

The blanks for tensile specimens were cut from the as received sheet parallel to the rolling direction as shown in Figure 3.1.

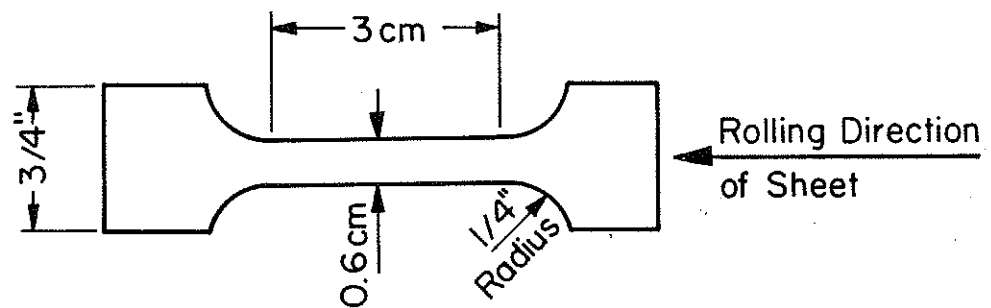


Fig. 3.1 Blanks for Tensile Specimens.

They were solution treated and quenched and immediately placed in the oil bath to age. At the appropriate aging times the specimens were removed from the oil bath and polished with 600 grit sand paper. They were then tested in tension to failure on an Instron Universal testing machine. The strain rate was 2.76×10^{-4} /sec. From each test the 2% offset yield strength and elongation to failure was recorded.

To establish the aging kinetics of the deformed material the procedure was slightly different because the material had to be cut into a tensile specimen after the deformation took place. The material was first cut into 3/4" strips and solution treated and quenched. It was then deformed as described in 3.22 before being placed in the aging baths. Again at appropriate times the specimens were removed and cut into tensile specimens, polished and mechanically tested. It should be noted that each specimen was deliberately made longer than the required length for a tensile specimen. This was to allow a piece of each to be labeled and stored in liquid nitrogen for future examination in the electron microscope.

3.3. Structural Examination

The structure of the thermal mechanical treated material was studied by optical, X-ray and electron metallography.

3.3.1. Optical Microscopy

Optical microscopy was used to find the grain size in the material. Specimens were solution treated at 500°C and quenched. Another set was solution treated, quenched, deformed 10% and 30% and heated to 50° and 100°C for one hour. The specimens were polished to a 1 micron finish and etched in Keller's etch (1.0 ml HF, 1.5 ml HCl, 2.5 ml HNO₃, 95 ml H₂O) for 10 - 20 seconds. The grain size was then measured. There was no evidence of recrystallization after any of the treatments.

3.3.2. X-ray Diffraction Techniques

The Debye-Scherrer powder method was used for structural examination of the material. Rather than filing the material to produce a powder, approximately 1mm x 1mm rods were chemically polished in 200 grams per litre Na OH at 70°C, mechanically polished, and electropolished in 5% perchloric acid in methanol at < -20°C. This produced a needle that was immediately covered with vacuum grease and placed in the camera. Cu K α radiation was used with a Ni filter for various exposure times.

The method described above removed any reflections due to oxide on the film. However other than d-spacings attributed to the Aluminum matrix no diffraction effects were seen.

3.3.3. Electron Microscopy

The preparation of thin foils for structural examination in the electron microscope was achieved in two ways. First the material that did not have to be deformed after solution treatment was rolled to .015 → .020 cm. before any heat treatment was applied. After the heat treatments the material was carefully mechanically polished with 600 grit sand paper on a flat surface and then a 3 mm disc was punched out. To make a thin foil of the 3 mm disc the STRUERS TENUPOL jet polishing technique was used with an electrolyte of 5% perchloric acid in methanol at a temperature of -60°C. The specimens were polished at 9-V for various lengths of time depending on the exact thickness and heat treatment of the disc. When a hole appeared the disc was quickly emersed in methanol, washed in ethanol, dried between filter papers and placed in the electron microscope specimen holder.

The second type of preparation was for thin foils that were made from the bulk specimens, i.e., those that were deformed 10% and 30%. As this material was 0.7 to 0.9 cm thick it was polished chemically to approximately .020 cm before electropolishing. The chemical polish was 400 cc/litre HCl and 5g/litre NiCl₂ at room temperature. To achieve uniform polishing it is necessary to hold the specimen horizontally in the polishing solution. It is also necessary to cool the specimens in water periodically during the chemical polishing process. After chemically polishing to 0.02 cm a thin foil was prepared as in the first method.

4. EXPERIMENTAL RESULTS

The specimens were solution treated at 535°C in an air furnace for twenty four hours and quenched in water. The as-quenched structure of the specimens showed no precipitation. The solution treated specimens were aged at room temperature, 100°C, 150°C and 190°C and the aging kinetics at the various temperatures of aging were established by mechanical tests. Solution treated specimens were also deformed 10% and 30% by rolling at room temperature, 50°C and 100°C and aged at 150°C for various lengths of time. Again the mechanical properties were tested to establish the aging curves.

The structures of the precipitates were examined after various times and conditions of aging using selected area diffraction and dark field techniques. Dislocation structures in the deformed materials were examined to study the effect of various thermo-mechanical treatments on the defect structure of the specimens.

The results of these studies will be presented in two sections, one on the mechanical properties and the second on the structure of thermo-mechanically treated specimens.

4.1. Mechanical Properties

The mechanical properties of the undeformed materials are shown in Figure 4.1 and 4.2. The specimens aged at room temperature do not achieve a maximum strength even after 3200

hours aging. The curve appears to level at approximately 27,000 psi. Elongation of the room temperature aged material falls to approximately 24% from the 31% of the solution treated material and also levels off.

The aging kinetics of Al 2036 for 100°C, 150°C, and 190°C could be said to display normal aging behaviour i.e., as the aging temperature is reduced the time required to attain maximum strength and the strength reached at this maximum are increased. This is shown in Figure 4.2 for the 190°C and 150°C cases where 41,000 psi at 20 hours and 46,500 psi at 170 hours are the maximums respectively. As shown in Figure 4.1. at 100°C the yield strength of the aged specimens rises steadily up to 1000 hours of aging, however, after that it begins to rise dramatically. Due to time constraint specimens were aged for only up to 2,000 hours at 100°C.

The percent elongation to fracture of all three aging treatments follows a definite trend. As the strength of the material begins to rise sharply to a maximum the elongation decreases sharply. The elongation then tends to level off during the period of maximum strengths. Contrary to what one would expect as the material becomes overaged the elongation again takes a downward turn. This is best exemplified in the 150°C elongation curve.

The mechanical properties of the deformed material aged at 150°C are shown in Figure 4.3 and Fig. 4.4. It can be seen in both cases that increasing the temperature of

deformation from room temperature $\rightarrow 50^{\circ}\text{C} \rightarrow 100^{\circ}\text{C}$ also increases the maximum yield strength of the material. Figure 4.5, Figure 4.6 and Figure 4.7 show that increasing predeformation from 10% \rightarrow 30% also increases the maximum yield strength on aging at 150°C .

It should be noted that in all cases of predeformed material being aged there is a definite drop in strength in the early stages of aging. Upon further aging this drop is overcome before maximum strength is attained.

The elongation of the predeformed material follows virtually identical paths in all six cases. There is an increase in the first hour of aging that corresponds to the early decrease in strength. The elongation then drops off slowly to a very level curve through the times of maximum strength and into the overaged conditions. It should be noted that while the strength of the material is definitely increasing with increasing predeformation temperature the change in elongation is almost negligible. This is contrary to normal behaviour i.e., normally as the strength goes up ductility goes down. However as the temperature of predeformation is increased the value of peak strength on aging goes up but ductility remains practically the same.

The times required to achieve the maximum strengths are clearly affected by the amount of predeformation. In the undeformed material maximum strengths at 150°C aging were attained after approximately 170 hours. The maximums

were attained in the 75 → 100 hour range for 10% deformation and in the 50 → 75 hour range for 30% deformation.

4.2. Structure of Thermo-Mechanically Treated Specimens

4.2.1. Solution Treated and Deformed Specimens

In preparation for aging, the specimens were solution treated or solution treated and deformed. The solution treated specimens contained a very uneven distribution of a hexagonal particle range from 600Å to 1500Å in size. These hexagonal particles persisted in foils of variously heat treated specimens and their size was always of the same order of magnitude (Figure 7.1A and Figure 7.1B). The d-spacing of this particle was extremely large (~ 12Å) and was not consistent with any of the major hardening precipitates expected to form in this alloy. The actual structure of the hexagonal particle could not be obtained. No other diffraction effects or precipitates were seen in solution treated foils.

As the trends in changes in mechanical properties were consistent through raising the deformation temperature from room temperature → 50°C → 100°C only the extremes of room temperature and 100°C were studied with the electron microscope. The same is true for the amount of deformation. the 30% deformed state simply exaggerates any effects found in the 10% deformed state.

The solution treated and deformed foils gave no indication of precipitates other than what was observed in

the solution treated condition. However, immediately after deformation the dislocation substructure is observed to be dependent on the temperature of deformation and the amount of deformation. The specimens deformed at room temperature have a cellular type of structure (Figure 7.2 and Figure 7.3). The cells of the material deformed 30% appear to be smaller and have a higher dislocation density in the cell walls.

The specimens that were deformed at 100°C have no indication of cellular structure. The dislocation substructure is very even and finely distributed throughout the foil. It can be seen by comparing Figure 7.4 and Figure 7.5 that the specimen deformed 30% has not only a more dense but a finer distribution of dislocations.

4.2.2. Aged Specimens

The precipitate structures and dislocation structures were observed in the undeformed and aged and in the deformed and aged specimens. Times of aging were related to the aging curves produced by mechanical testing to have specimens in the underaged, maximum strength and overaged conditions.

Undeformed specimens aged at room temperature showed no precipitates or diffraction affects other than those attributed to the hexagonal particles mentioned earlier. Aging to 3200 hours at room temperature (Figure 7.1B) did not produce any precipitation visible in the electron microscope.

Undeformed specimens aged at 150°C which reached a

maximum strength at approximately 170 hours allowed a definite determination of the strengthening precipitates. After 70 hours at 150°C (Figure 7.6) there is the formation of small spherical particles in the range of 100Å → 200Å. Diffraction effects are ambiguous at this stage but structural examination of specimens aged for longer periods of time suggest that these could be GP₂ zones. Continuing aging to maximum strength, for 170 hours, shows (Figure 7.7 and Figure 7.8) a very definite and extremely dense precipitate structure. The precipitates are thin needles lying perpendicular to each other. Diffraction effects from foils of this specimen (Figure 7.9) are in exact agreement with the d-spacing of θ' for the 011 and 110 reflections as documented by Thomas and Whelen⁽¹⁵⁾. The orientation relationship of θ' with the matrix is (001)_m//(001)_{θ'}. The extreme streaking in the < 001 > directions in reciprocal space agrees with the conclusions⁽¹⁵⁾ that the θ' precipitates lie on the (001) planes of the aluminum matrix. On aging at 150°C for 500 hours it is seen (Figure 7.10) that the precipitates increase in size from about 900Å at maximum strength to about 2000Å in the overaged condition. The increase in size is apparently at the expense of the smaller precipitates as the density of precipitates seems to decrease. A loss in mechanical properties follows this growth.

A specimen was aged for 165 hours at 300°C. The structure of this specimen in bright and dark field is shown

in Figure 7.11A and Figure 7.11B respectively, whereas the selected area diffraction pattern is shown in Figure 7.12. The diffraction pattern due to θ is superimposed on the (011) pattern of the aluminum matrix. The complete indexing is shown in Figure 7.12. The orientation relationship of θ with the matrix is

$$(\bar{1}10)_{\theta} // (00\bar{1})_M$$

The dark field shown in Figure 7.11B is due to $(\bar{2}20)_{\theta}$ reflection which is very close to $(00\bar{2})$ reflection due to the matrix. This dark field picture shows the presence of θ precipitate. This also suggests the precipitation reaction in this alloy follows a sequence similar to those observed in Al-4% Cu alloy.

Aging of deformed specimens at 150°C affected the dislocation substructure. During the initial stages of aging after deformation there is a loss of strength in all conditions. Figure 7.13 shows that the dislocation density of a specimen 30% deformed at 100°C seems to drop in the first hour of aging. Figure 7.14 shows that a specimen deformed 30% at room temperature and aged 1 hour has better defined cell boundaries that suggest some recovery is taking place. It should also be noted in Figure 7.13 that hexagonal particles of the same order of magnitude as Figure 7.1B are clearly visible. This strengthens the belief that these particles do not grow on aging.

The loss of dislocation density does not seem to continue on further aging. Specimens that have been aged 50 hours after 30% deformation at room temperature and 100°C retain virtually all of the dislocation structure seen after 1 hour of aging.

Examination of specimens aged to their maximum strengths reveals (Figure 7.15) that not only is the dislocation structure retained but a dense and evenly distributed precipitate structure can also be seen. The precipitate structure of the deformed material was identified to be θ' using electron diffraction patterns. That is, in both deformed and aged, and solution treated and aged specimens the strengthening precipitate was observed to be θ' . Precipitate size in material deformed 30% at 100°C and aged at 150°C for 75 hours is comparable to precipitates in the undeformed material aged at 150°C for 170 hours.

Again at 190°C, material deformed 30% at 100°C, produced much the same effects as aging deformed material at 150°C. After 2.5 hours the precipitates were not visible in bright field because of the dislocation substructure (Figure 7.16). However a dark field micrograph (Figure 7.17) shows the formation of small θ' precipitates has already started. After 23 hours at 190°C which is close to the maximum strength a very ordered and finely distributed precipitate structure was seen (Figure 7.18). The diffraction patterns were similar to those of θ' seen when the specimen was aged at 150°C.

Again it was possible to index the $0\bar{1}1$ and 110 reflections of the θ' precipitate. Continuing aging at 190°C to an overaged condition of 188 hours allowed clear micrographs to be taken of the precipitate structure. Figure 7.19 and Figure 7.20 taken in the (001) foil normal show the precipitate morphology to be virtually identical to that of the maximum strength conditions except the precipitates have grown slightly. The orientation relationship of θ' with the matrix is identical in the predeformed material and the solution treated material.

Figure 4.1. Aging and Elongation Curves of Undeformed Material
Aged at 100°C and Room Temperature

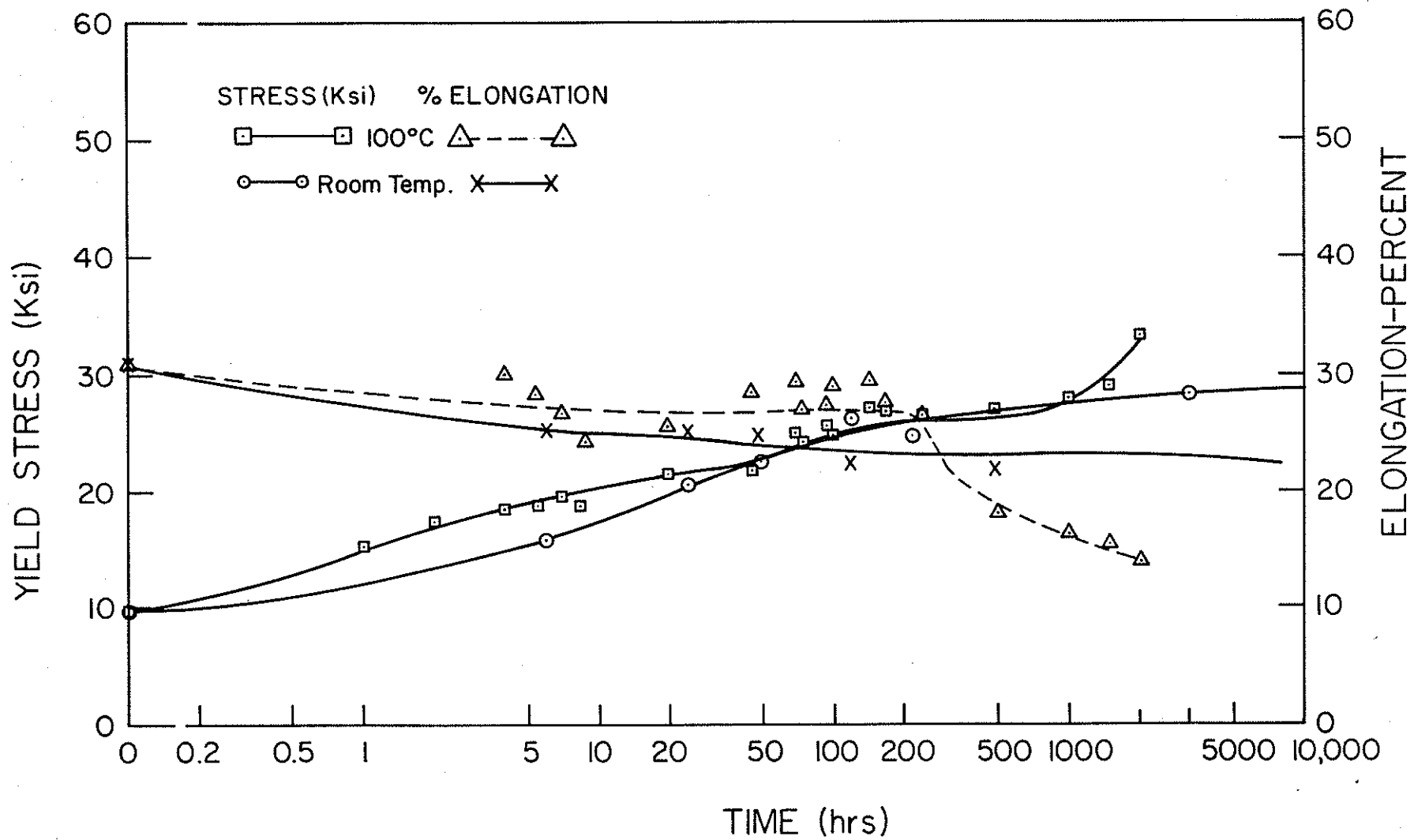


Figure 4.1 Aging and elongation curves of undeformed material aged at 100°C and room temperature.

Figure 4.2. Aging and Elongation Curves of Undeformed Material aged at 150°C and 190°C.

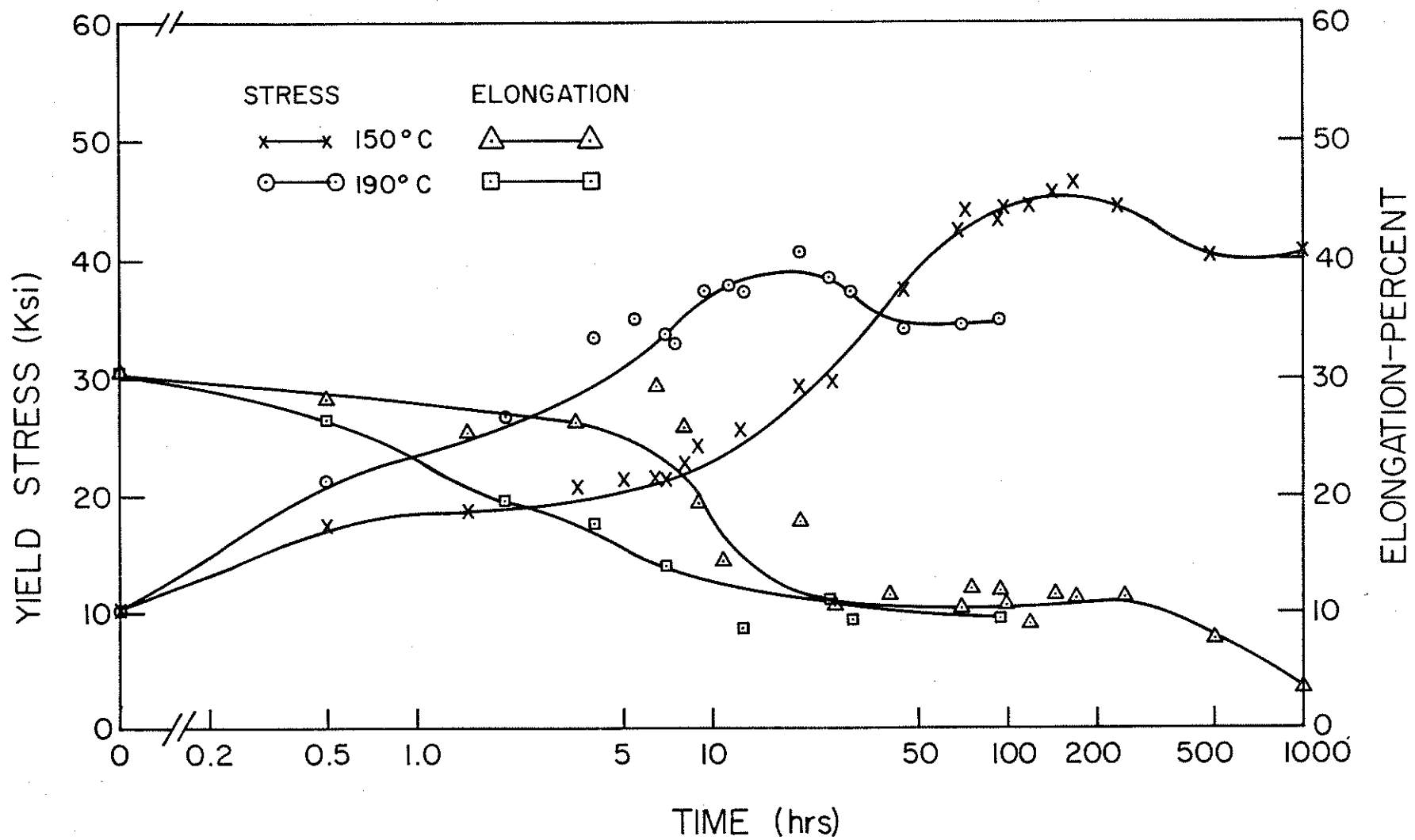


Figure 4.2 Aging and elongation curves of undeformed material aged at 150°C and 190°C.

Figure 4.3. Aging and Elongation Curves of Deformed Material aged at 150°C. 10% Deformation at Room Temperature, 50°C, and 100°C.

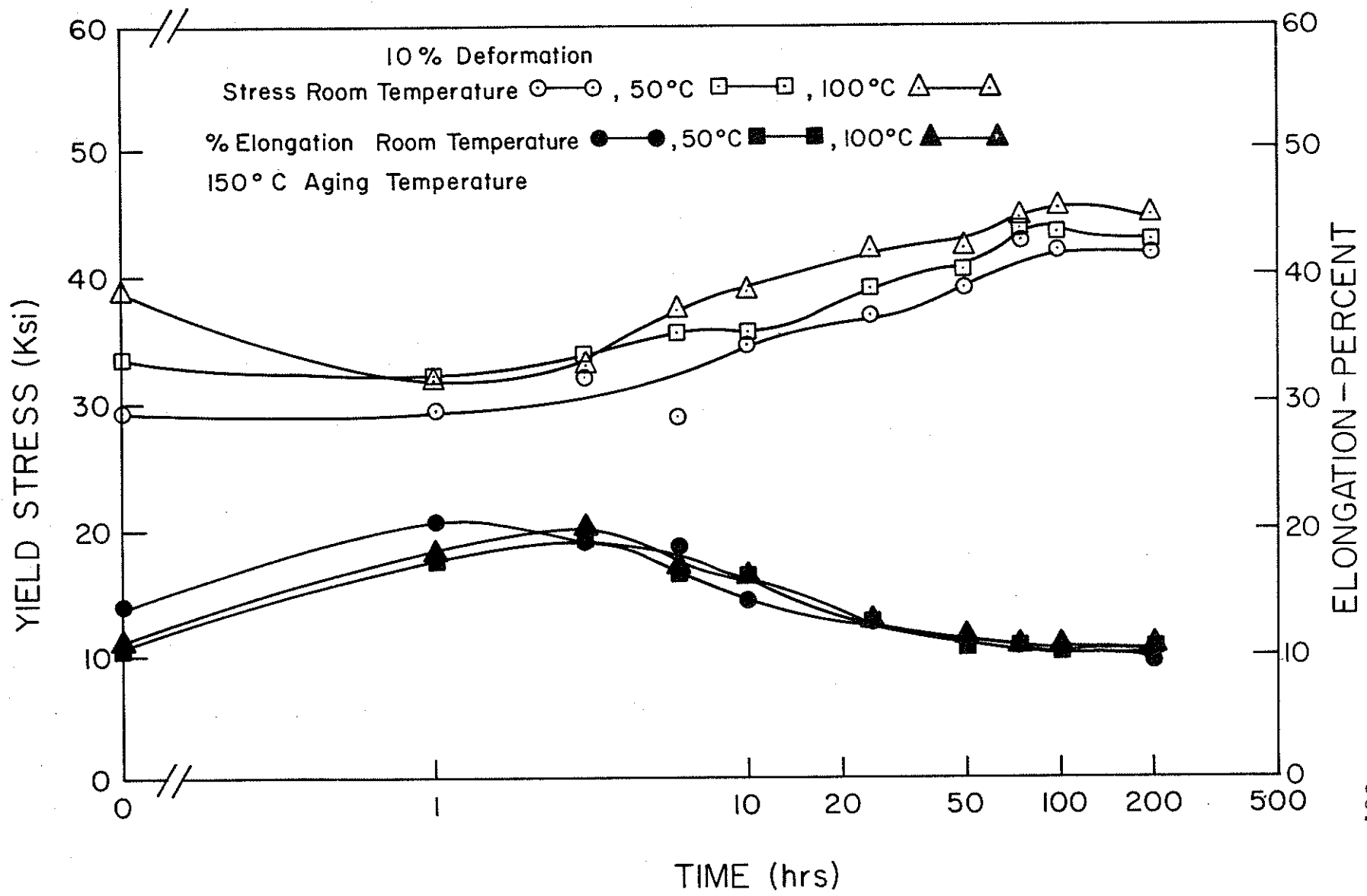


Figure 4.4. Aging and Elongation Curves of Deformed Material
Aged at 150°C. 30% Deformation at Room Temperature,
50°C, and 100°C.

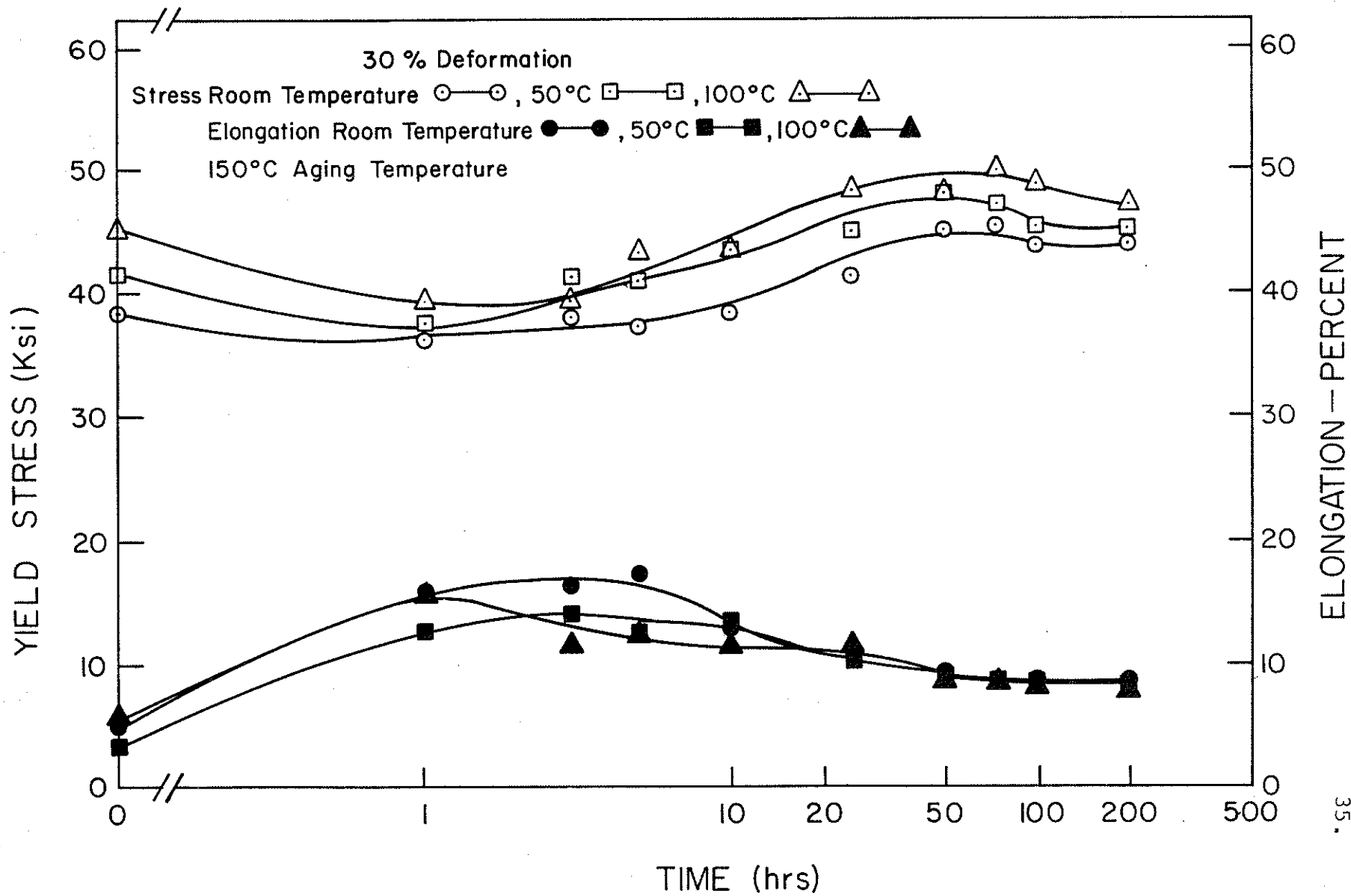


Figure 4.5. Aging Curves of Material Deformed 10% and 30%
at room Temperature.

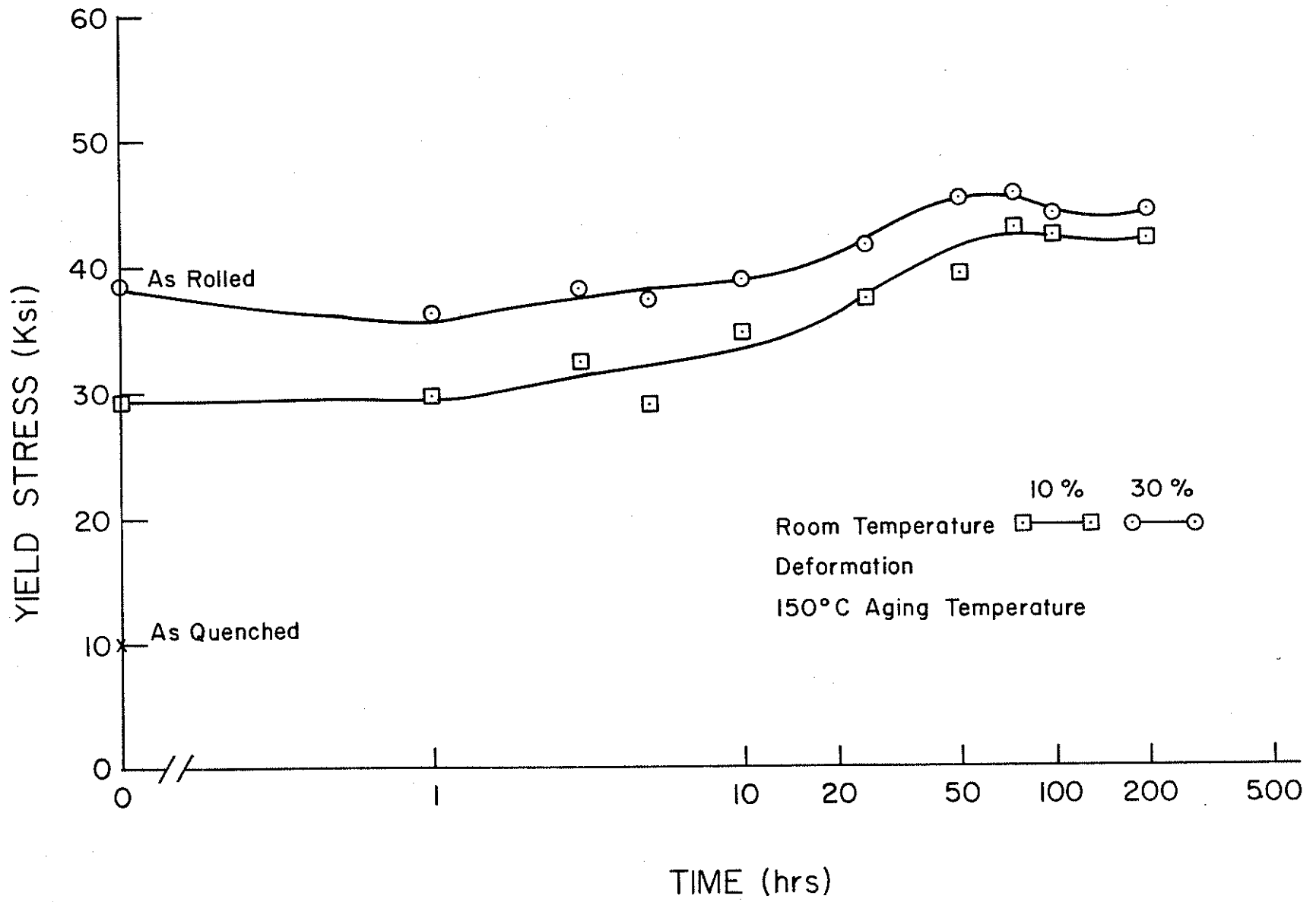


Figure 4.6. Aging Curves of Material Deformed 10% and 30%
at 50°C.

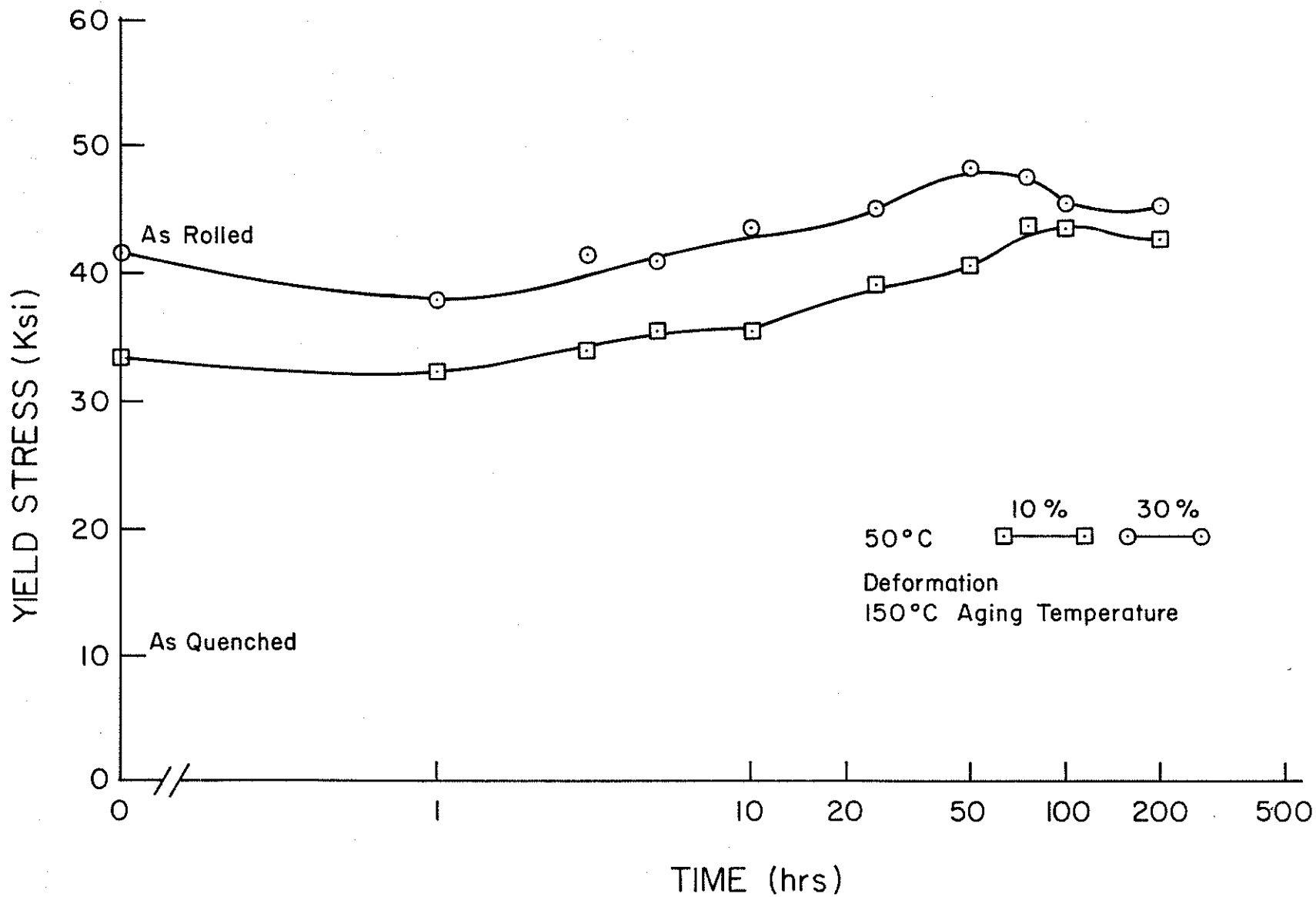
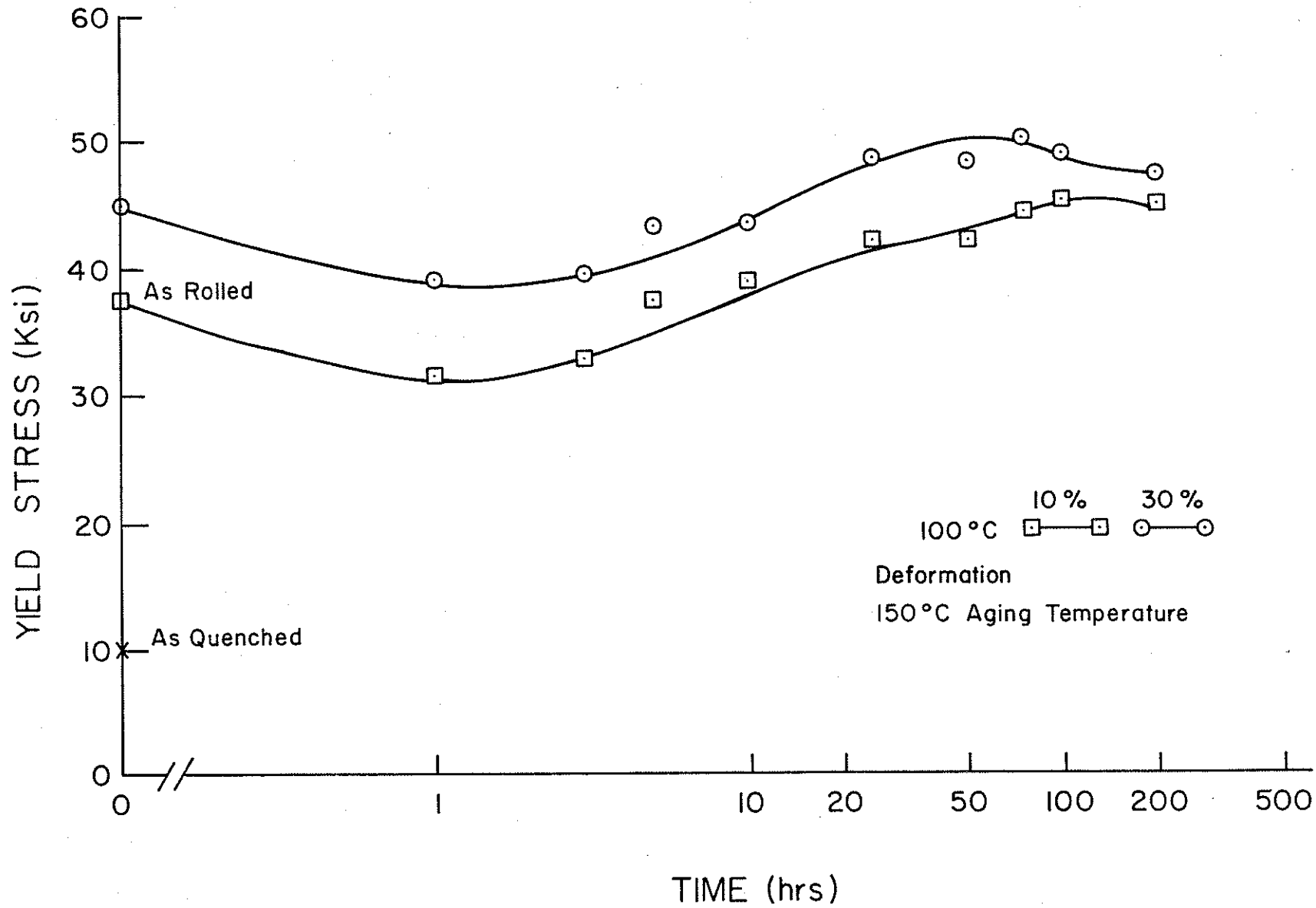


Figure 4.7. Aging Curves of Material Deformed 10% and 30% at 100°C.



5. DISCUSSION OF RESULTS

This project was undertaken to study the effect of thermo-mechanical treatment on the mechanical properties of Aluminum 2036 alloy. In this section an attempt will be made to explain the results obtained and the relationship between the structure and the mechanical properties of the thermo-mechanically treated specimens.

The effect of prior deformation upon aging at 150°C is shown by Figure 5.1. The 10% prior deformation results in lower maximum yield strengths than non-deformed material with only a slight decrease in optimum aging time. However, 30% prior deformation results in increased maximum yield strength over the non-deformed material and a decrease in optimum aging time from 170 hours to 50 hours. The decrease in maximum yield strength at room temperature and 50°C deformation could be attributed to the heterogeneous nucleation of precipitates in the dense cell walls of the dislocation structure. This would mean that the centre of the cells would not only be weakened by a lower dislocation density but also by a lower density of precipitates. As the cell structure of dislocations does not form at 100°C deformation, there is still a uniform nucleation of precipitate along with the dislocation substructure and the maximum strength is increased.

The effect of temperature of prestrain on the mechanical properties is shown in Figure 4.3 and Figure 4.4. In either case of 10% or 30% deformation when the temperature of pre-

strain was increased from room temperature $\rightarrow 50^{\circ}\text{C} \rightarrow 100^{\circ}\text{C}$ the yield strength increased. The increment of strength was attained immediately after the deformation and was retained through all stages of the aging curves.

The immediate increment in strength is attributed to the formation of a dense location substructure at the 100°C deformation in contrast to a cellular type of structure seen in the material deformed at room temperature. The cellular type of structure is typical of low temperature ($< 0.4 T_m$) deformation of materials with stacking fault energy high enough to allow the processes of cross slip to take place. At strains less than 1% straight dislocations are produced which interact with one another to form closeknit grids resembling nets. Continued deformation causes profuse multiplication and clustering of dislocations into tangles. These

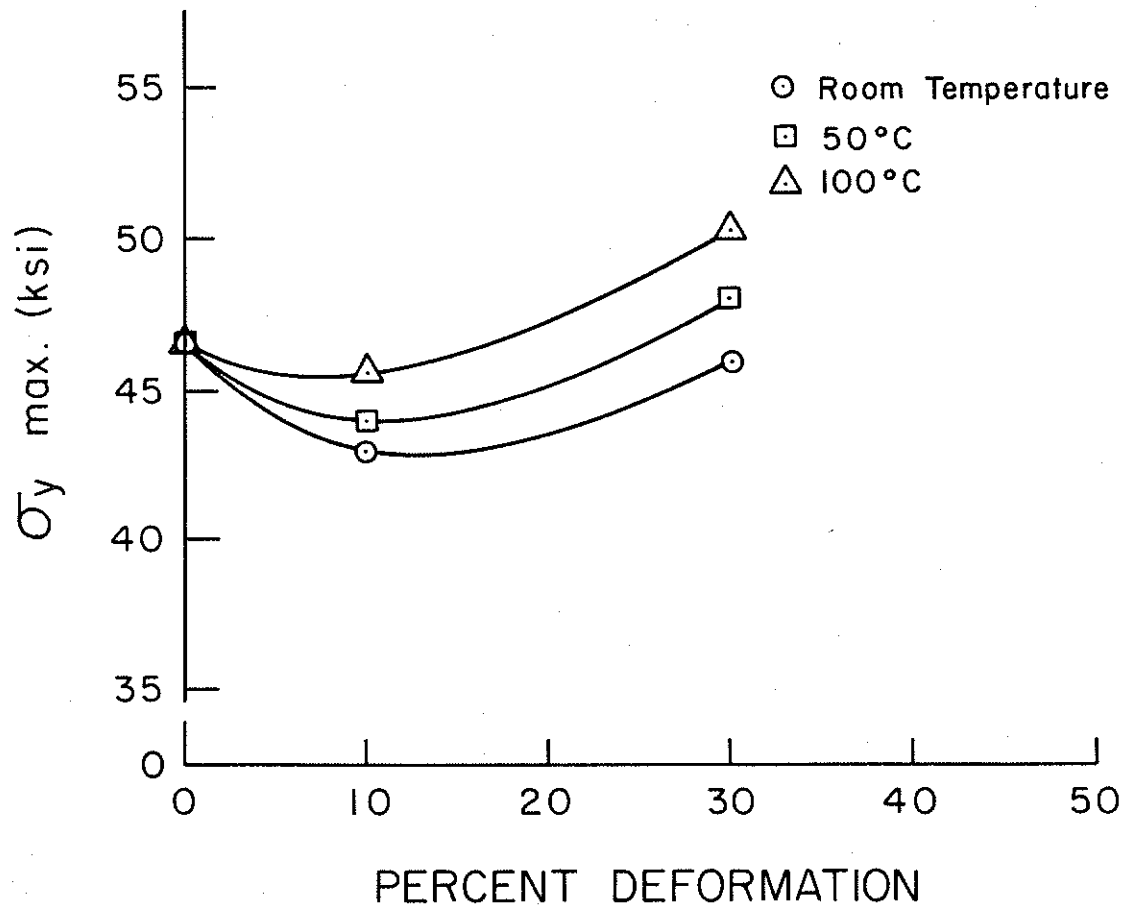
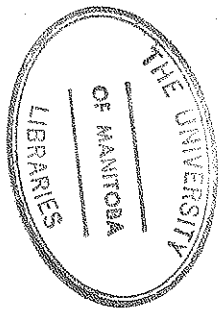


Fig. 5.1 The σ_y Max. at 150°C Aging vs. Percent Deformation at Various Temperature .

tangles grow in number and in size until at approximately 10% strain the tangles link up into a fairly well defined cell structure⁽¹⁾. The cells are characterized by cell walls of high dislocation density. The increase in strength in the material with more even dislocation distribution is in agreement with work done by Carrington et al⁽²⁾ that says the flow stress is directly related to the cell interior dislocation density through equation (1). Therefore despite the high density in the cell walls of the material deformed at room temperature it is the more evenly distributed substructure of the 100°C deformed material that at least partially results in higher strengths.

The dislocations in the specimens deformed at elevated temperatures were seen to be uniformly distributed. This observation is similar to those observed when a material is deformed in the temperature region of serrated yielding⁽⁹⁾. Aluminum alloys are known to exhibit the effects of serrated yielding in the temperature region of 50°C + 100°C⁽²⁵⁾. This temperature region is dependent on the strain rate. Although the strain rate during deformation by rolling was not calculated it is likely that serrate yielding was taking place during deformation which would give rise to the uniform distribution of dislocations observed in the specimens deformed at 100°C.

Another possibility for the increment in strength of the material deformed at 100°C could be due to the precipit-

ation at 100°C during deformation. Although these precipitates were not observed in the electron microscope, as they may be extremely fine, but may be large enough to lock up dislocations and cause an increase in strength.

The early stages of aging show a drop in strength and an increase in ductility in all conditions of the predeformed material. The drop in strength is the result of recovery taking place in the dislocation substructure at a greater rate than the rate at which the nucleated precipitates can affect the strength. As the precipitation progresses the recovery and recrystallization of the material may be impeded which would prevent softening and yield strength would start to increase, i.e., a minimum in the aging curve would occur. Past this point the effect of the precipitates is to stabilize the structure and the strength of the material increases.

The increase in strength of specimens due to an increase in the temperature of deformation seems to have been maintained throughout the aging process at 150°C. This may also be due to the effect of more uniform dislocation distribution that is formed in the material by deformation in the dynamic strain aging region. The effects of this type of treatment should continue to improve the material properties with increasing temperature of predeformation as long as it remains in the dynamic strain aging region.

The precipitate structure and kinetics of aging are apparently affected by the temperature of aging and amount

of predeformation more than the temperature of predeformation. An attempt will be made to explain the effects of these variables in relation to the observed results.

The undeformed material aged at room temperature never achieves a maximum strength and the strength that the curve levels off at is well below the maximum strengths attained at higher aging temperatures. This is consistent with structural examination that shows the formation of θ' does not take place even at aging time of 3200 hours. Although there were no diffraction effects other than those attributed to the hexagonal particles it is obvious that some hardening mechanism must be responsible for the increment in strength. Thomas and Whelan⁽¹⁵⁾ attribute low temperature aging effects to zones of plate like clusters of copper atoms. The major strengthening precipitate in the Al-Cu alloy system is θ' and the optimum strength can only be achieved under conditions where θ' is formed.

The hexagonal particle does not have any effect on the aging kinetics. It is apparently an undissolved inter-metallic compound that remains in the solution treated material and does not grow on aging. Some form of iron silicate or aluminum silicate could be the structure of these particles but the actual structure could not be established.

Aging undeformed material at 150°C shows small spherical particles in the early stages of aging as seen in Figure 7.6. These could be GP_2 zones as described by Nicholson and

Nutting⁽¹⁶⁾. The structure of precipitates at a comparably early stage of aging at 190°C but after predeformation appears to be the very early stages of the θ' precipitate (Figure 7.17). This is consistent with work done by Tavossoli⁽⁵⁾. His work showed that not only does predeformation cause a refinement of the precipitates but that the preferential nucleation of the intermediate precipitate that is responsible for maximum strength is at the expense of the formation of G.P. zones.

Another apparent difference arises in the overaged structures of the undeformed and deformed materials. In both cases the precipitate remains θ' however the relative growth of the precipitate is notable. The undeformed overaged material shows very large needles of precipitate while a comparably deformed and overaged specimen retains, except for slight growth, the fine distribution of precipitation seen in early stages of aging.

The effect of prestrain on the precipitate structure is best discussed relative to the aging kinetics at 150°C. The maximum strength is achieved in progressively shorter aging times as the material condition changes from no deformation \rightarrow 10% \rightarrow 30%. The temperature at which the deformation takes place appears to have little or no effect on the aging kinetics of the precipitate. In the early stages of aging the deformed material at 150°C the first diffraction effects are characteristic of the θ' precipitate. It appears that,

as in the 190°C case, the preferential nucleation of the θ' precipitate is accelerated by the amount of predeformation. This can be explained by the substantial increase in dislocation density caused by the increase in deformation. The strain fields in the crystal lattice caused by the dislocations accommodates the strain energy that has to be overcome to nucleate a precipitate in a perfect crystal lattice. The misfit of the intermediate θ' precipitate is greater than the misfit of G.P. zones. When the higher strain energy is accommodated by the dislocations, the nucleation is easier and the sites for nucleation increase with dislocation density. Therefore the increase of predeformation shortens the aging time to maximum strength by accelerating the formation of θ' precipitates.

The formation of $\theta(\text{Cu Al}_2)$ rather than $S(\text{Al}_2 \text{ Cu Mg})$ in Al 2036 is consistent with what would be expected in a commercial aluminum alloy with Cu:Mg ratio of 5.7:1. It has been shown by Tavassoli⁽⁵⁾ that the S precipitate could be expected with Cu:Mg ratio of approximately 2:1. However a Cu:Mg ratio of 4.5:1 shows no S formation and the precipitation scheme follows that of θ . It would seem reasonable that increasing this ratio further would retain the θ type of precipitation as there is relatively less Mg to form the ternary S type of precipitate. The work by Silcock⁽¹⁴⁾ that showed the concurrent formation of S and θ in a material with Cu:Mg ratio of 7:1 was done on pure laboratory

prepared material. It appears the impurities in a commercial material restrict the formation of the S precipitate.

CONCLUSIONS

1. The precipitated structure in aged Al 2036 is $\theta(\text{CuAl}_2)$.
2. The θ structure will only precipitate in large enough quantity to be detectible at high temperature aging (300°C).
3. Prestrain of the material accelerated the formation of θ' , which is the major strengthening structure, therefore shorting the aging times required to reach maximum strengths.
4. Prestrain in the dynamic strain aging temperature region will cause a more uniform dislocation structure and a finer distribution of precipitates.

SUGGESTIONS FOR FUTURE WORK

1. The electron microscope should be employed to look with more detail at the early stages of precipitation behaviour.
2. The effect of prestraining at higher temperatures on the mechanical properties and the structure of the precipitates.
3. The structure of the undissolved intermetallic compound seen in solution treated and aged specimens should be ascertained.
4. A detailed study of the complete aging sequence at one temperature should be studied.

6. REFERENCES

1. "Dislocation-Substructure-Strengthening and Mechanical-Thermal Treatment of Metals", R.J. McElroy and Z.C. Szkoziak, International Metallurgical Reviews, Vol. 17, pg. 167, (1972).
2. W. Carrington, K.F. Hale, and D. McLean, Proc. Roy. Soc., 1960, A, 259.
3. R.N. Wilson and P.G. Partridge, ACTA MET, Vol. 13, Dec. 1965, 1321.
4. Pashley, Rhodes, and Sendorek, Journal of the Institute of Metals, Vol. 94, 1966, pg. 41.
5. A.A. Tavassoli, Metal Science Journal, (1974), pg. 424.
6. J.M. Silcock, ACTA MET 8 (1960) 589.
7. Silcock, Heal, Hardy, Journal of the Institute of Metals, Vol. 84, 1955-56, 23.
8. P.G. McCormick, ACTA MET, Vol. 20, (1972) 351.
9. Lloyd and Tangri, Material Science and Eng., 10, (1972), 75.
10. J.G. Morris, Material Science and Eng. 16, (1974), 79.
11. C. Burdon and J.W. Martin, The Thermomechanical Treatment of a Al-Mg-Zr Alloy.
12. H.A. Lipsitt and C.M. Sargent and G.C. Weatherly, "Electron Microscopy and Structure of Materials", Thomas, Fulrath, Fisher, pg. 559.
13. H. Perlitz and A. Westgran, Arkiv Kemi, Min. Geol., 1943, B. Vol. 16, 13.
14. J.M. Silcock, Journal of the Institute of Metals, 1960-60, Vol. 89, pg. 203.
15. G. Thomas and M.J. Whelan, Phil. Mag., Vol. 6, (1960) page 1103.
16. Nicholson and Nutting, Phil. Mag., pg. 531 (1958).
17. Silcock and Heal, Acta Crystal, 9, (1956) 680.

18. B.A. Wilcox and R.I. Jaffee, *Trans. Japan, Inst. Metals*, 9, Supplement, 575, 1968.
19. D. Webster, *Trans. ASM*, 62, 936, 1969.
20. Thomas and Nutting: *The Mechanism of Phase Transformation in Metals*, p. 57, Institute of Metals, 1956.
21. R.N. Wilson, D.M. Moore, and P.J.E. Forsyth, *Journal of the Institute of Metals* 1967, Vol. 95, pg. 167.
22. R.N. Wilson and P.J.E. Forsyth, *Journal of the Institute of Metals* 1966, Vol. 94, pg. 8.
23. Matsuo and Hirhtu, *J. Japan Inst. of Light Metals*, Jan. 1975, 25, 18-23.
24. Screm and Palunlo, *Alluminio* 1971, 40, 595.
25. Worthington, *ACTA MED*, 1969, pg. 1357.

7. MICROGRAPHS

Figure 7:1A

Structure of the alloy 10% deformed at room temperature. The hexagonal particles undissolved in solution treatment are shown.

Figure 7:1B

Structure of material solution treated and aged 3200 hours at room temperature.

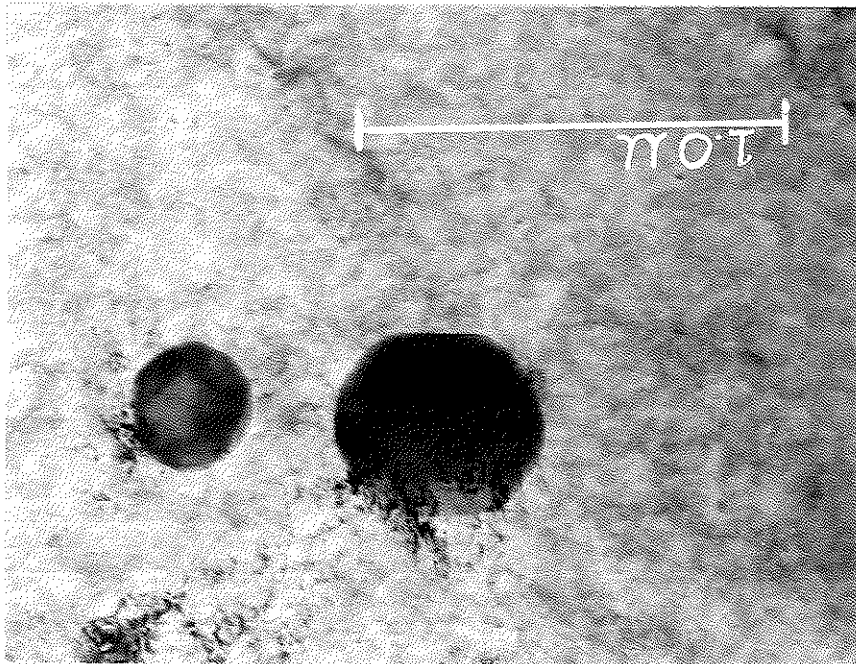
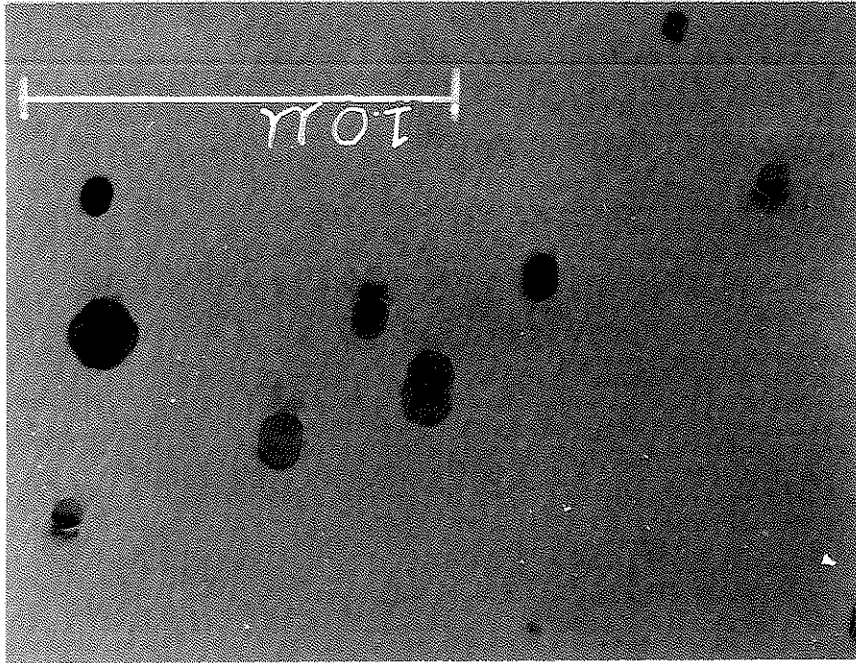


Figure 7:2

Cellular structure of material 30% deformed
at room temperature.

Figure 7:3

Cellular structure of material 10% deformed
at room temperature.

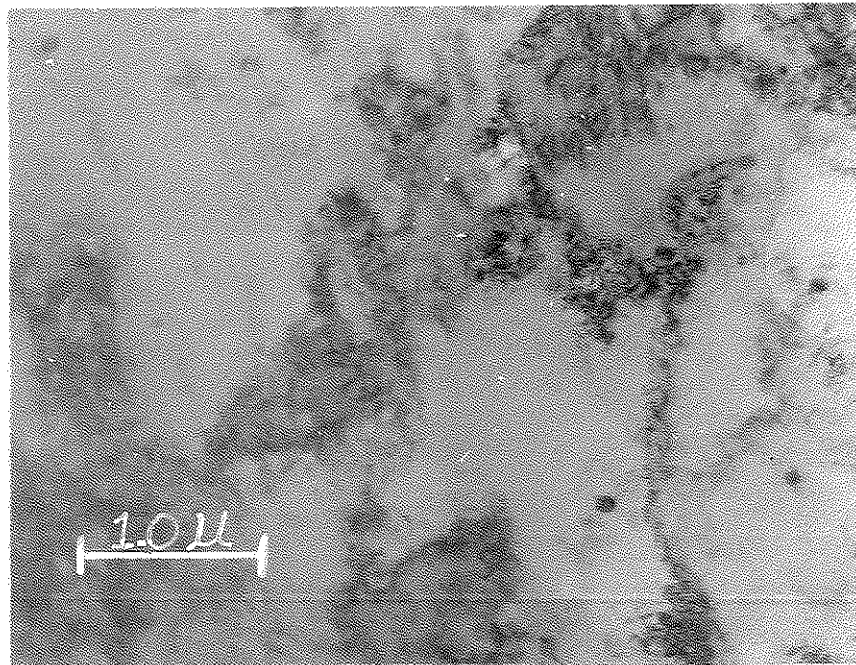
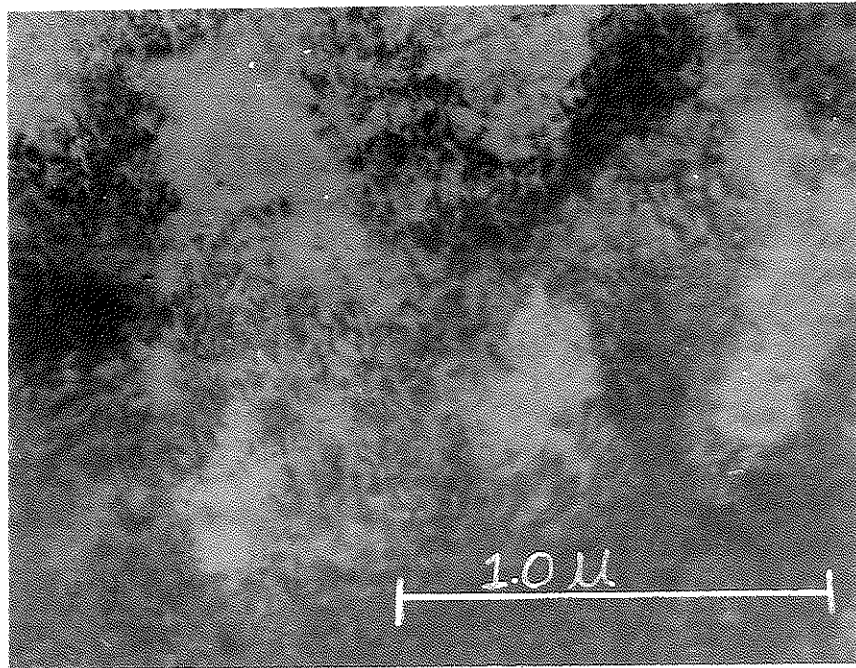


Figure 7:4

Structure of material 30% deformed at 100° C.

Figure 7:5

Structure of material 10% deformed at 100° C.

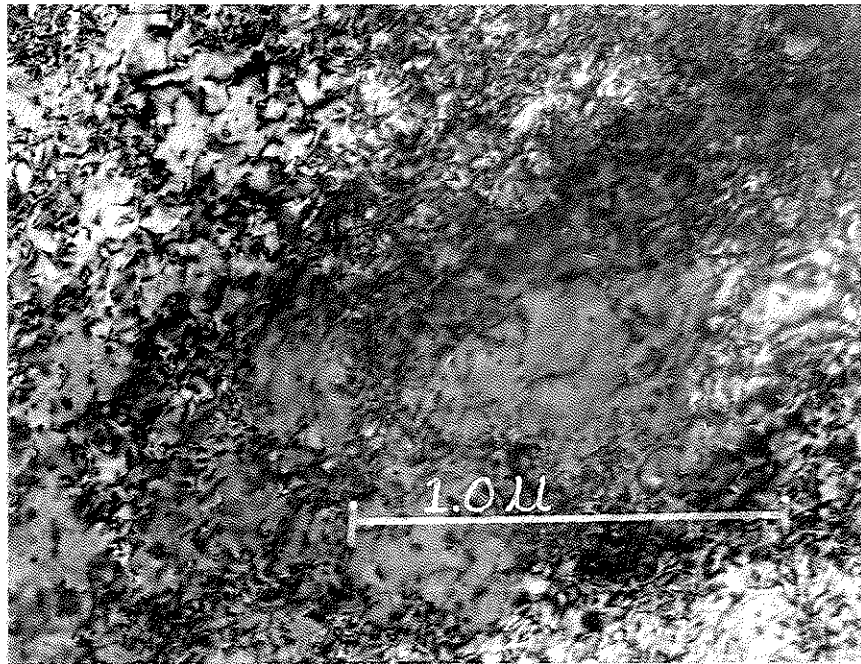
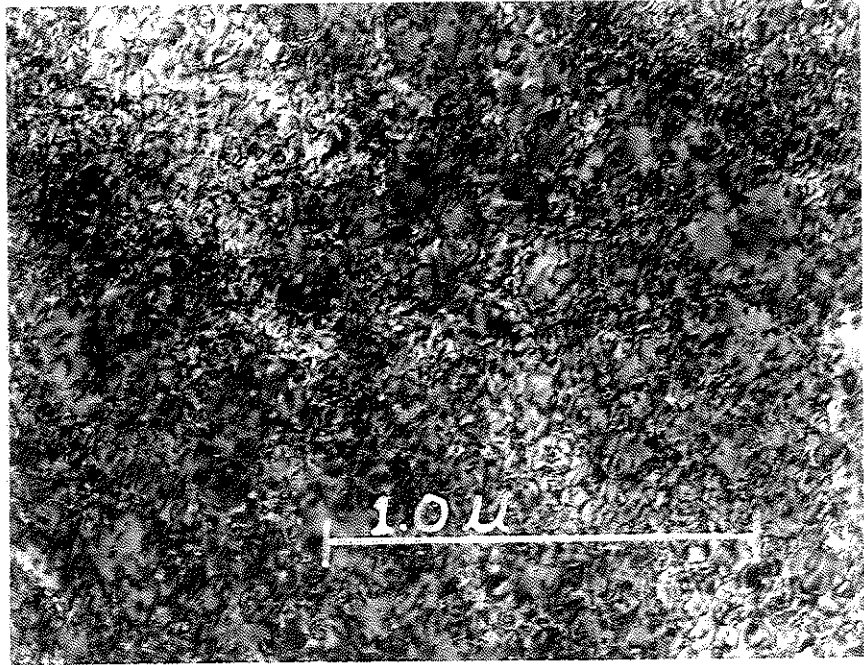


Figure 7:6

Structure of a specimen aged 70 hours at 150°C.

Figure 7:7

Structure of a specimen aged 170 hours at 150°C.

[(001) foil normal]

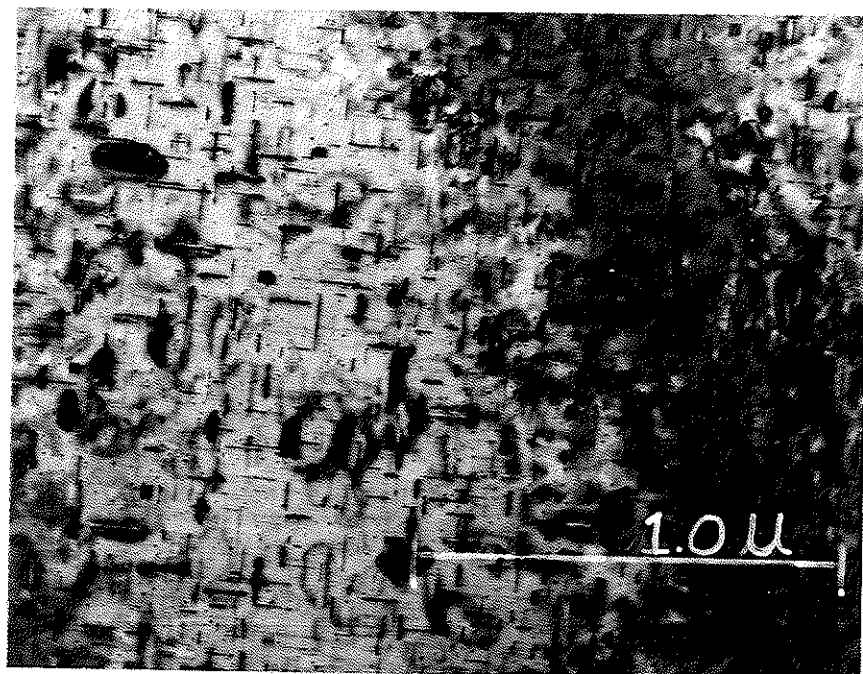
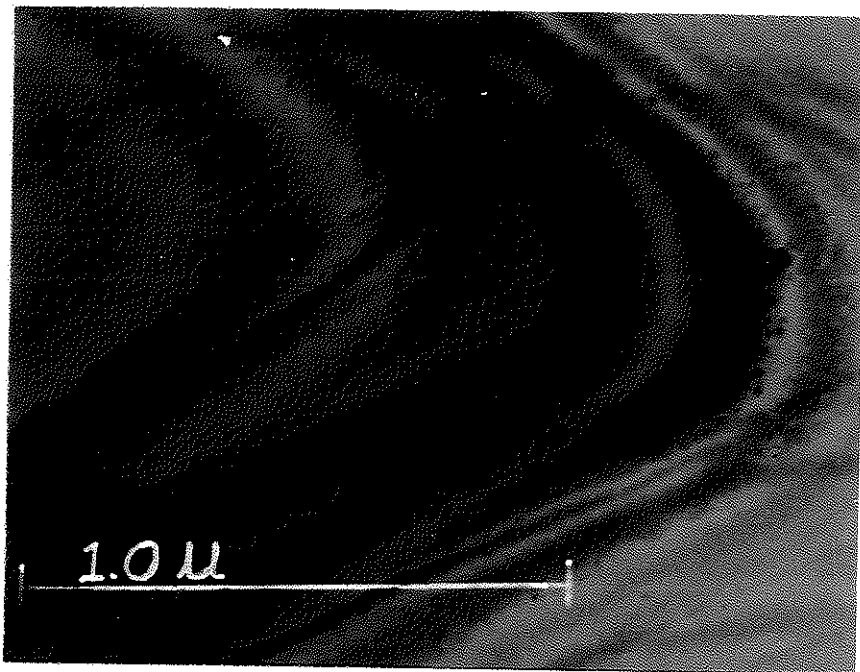


Figure 7:8

Structure of a specimen aged 170 hours at 150°C.

[(011) foil normal]

Figure 7:9

Selected area diffraction pattern of Figure 7:7.

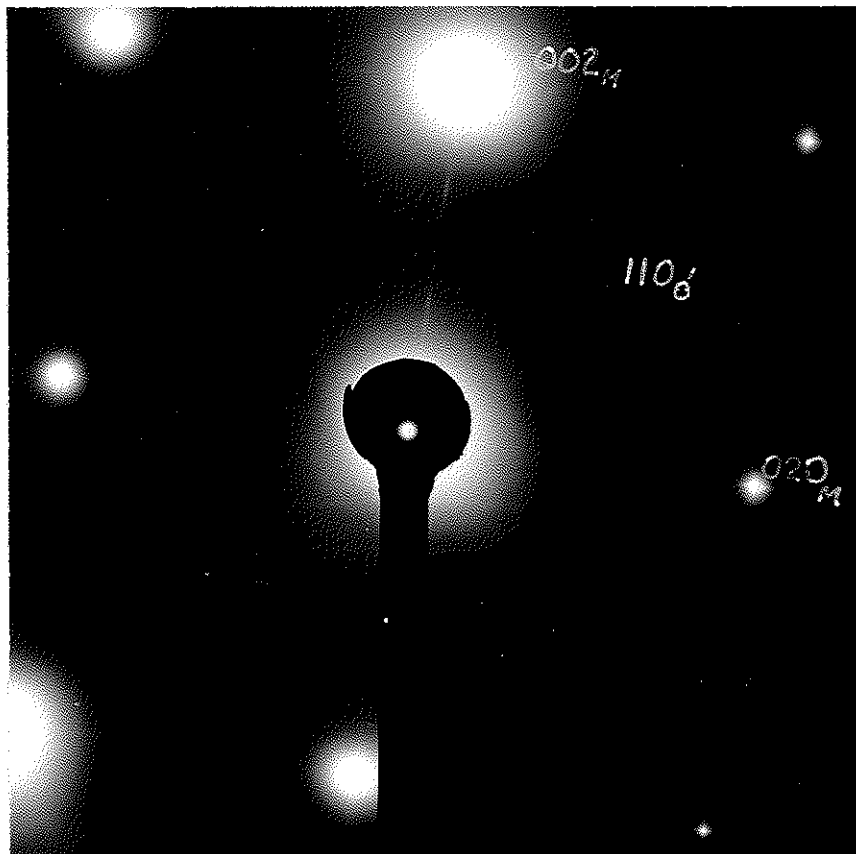
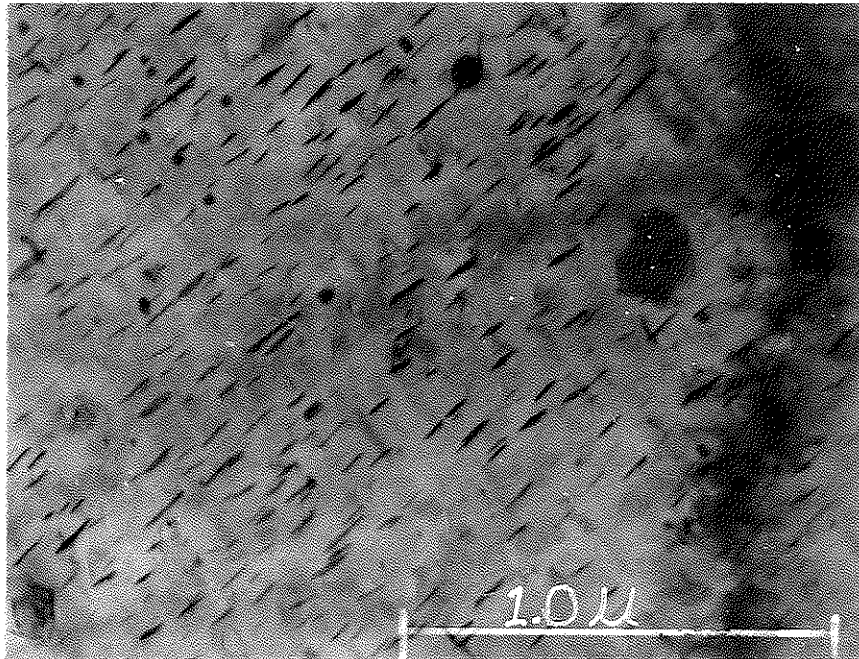


Figure 7:10

Structure of a specimen aged 500 hours at 150°C.

Figure 7:11A

Structure of material aged 165 hours at 300°C.

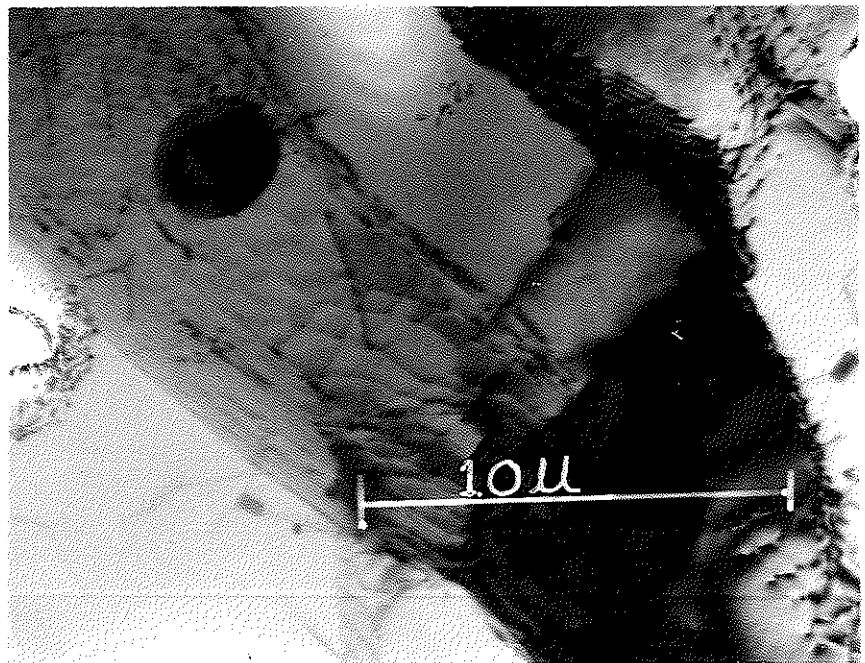
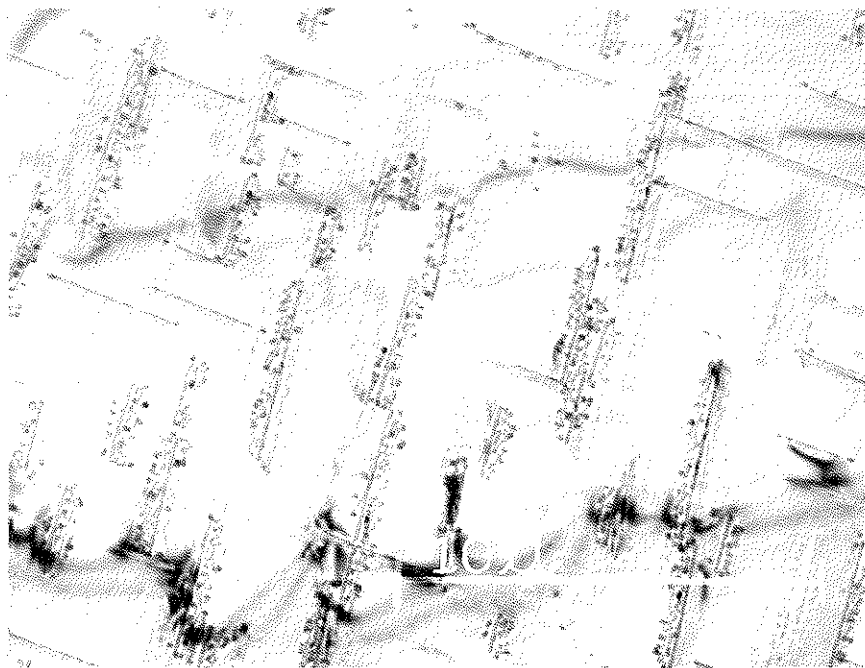


Figure 7:11B

Dark field of Figure 7:11A taken with (002)
diffraction spot.

Figure 7:12

Diffraction pattern of Figure 7:11.

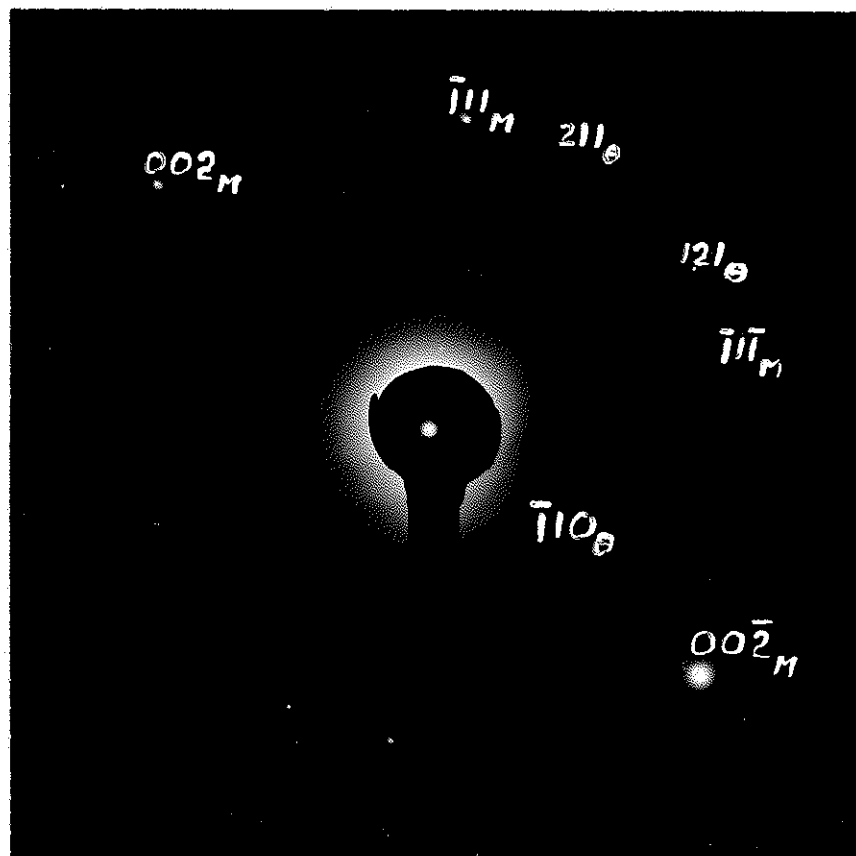
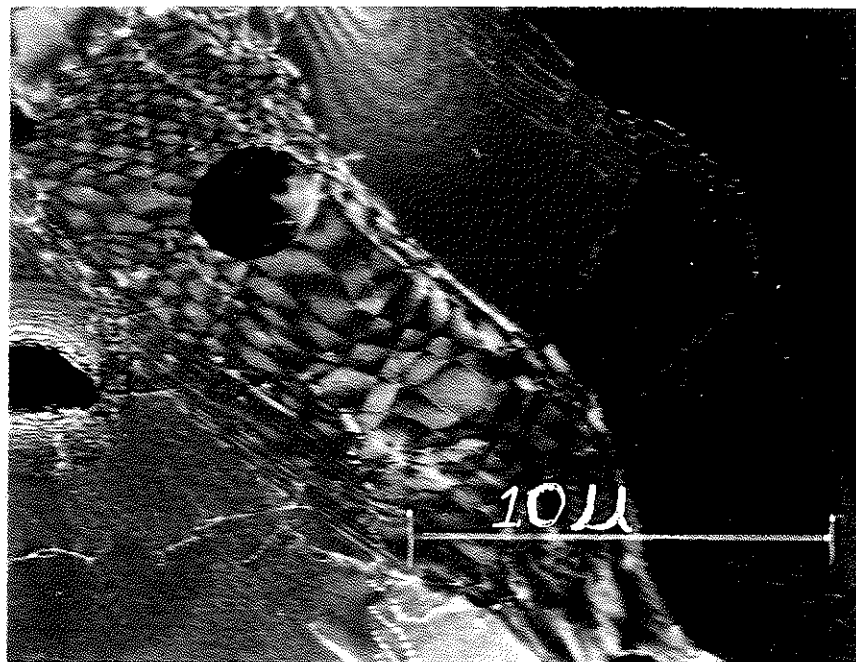


Figure 7:13

Structure of material 30%deformed at 100°C and aged 1 hour at 150°C.

Figure 7:14

Structure of material 30% deformed at room temperature and aged 1 hour at 150°C.

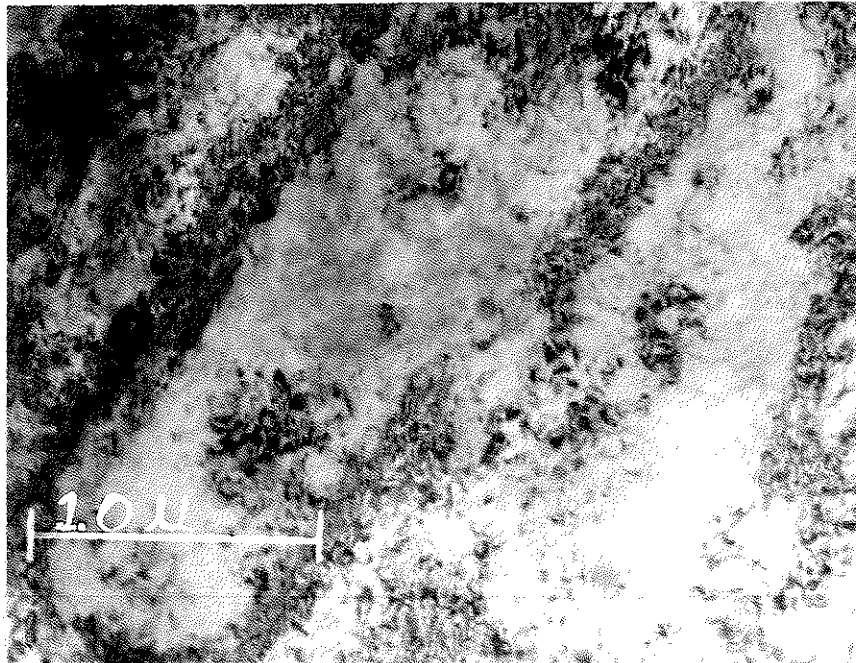
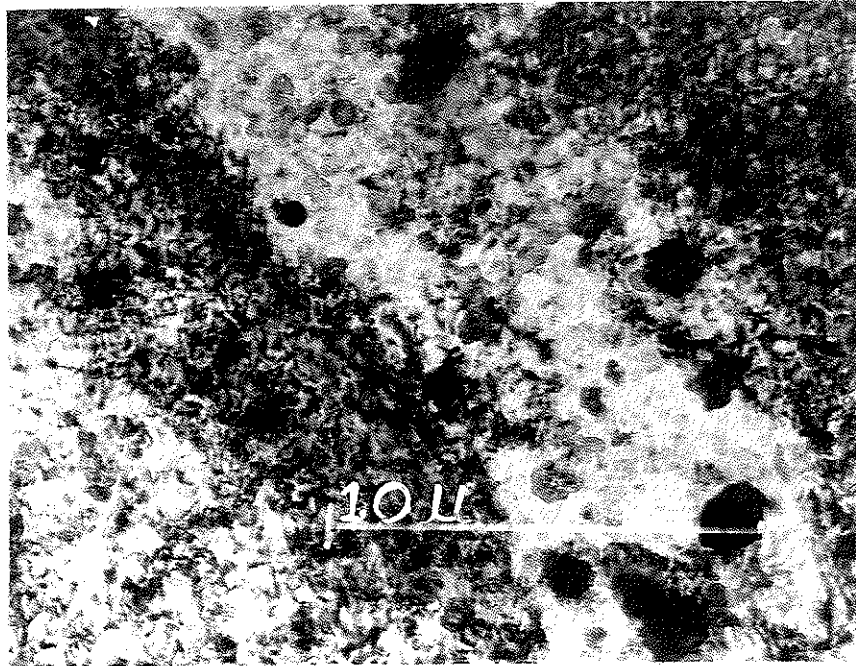


Figure 7:15

Structure of material 30% deformed at 100°C
and aged 100 hours at 150°C.

Figure 7:16

Structure of material deformed 30% at 100°C
and aged 2.5 hours at 190°C.

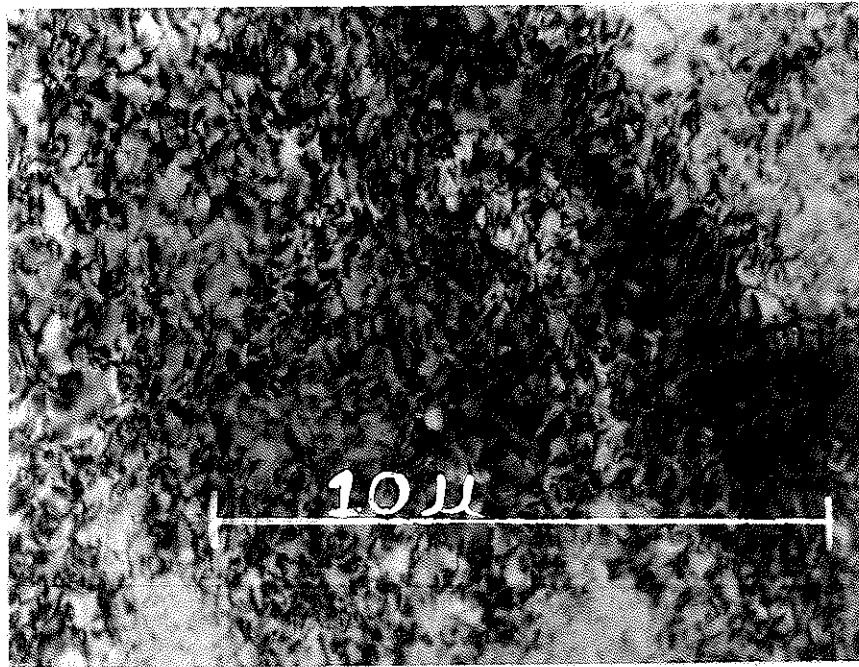


Figure 7:17

Dark field of Figure 7:16.

Figure 7:18

Structure of material deformed 30% at 100°C
and aged 23 hours at 190°C.

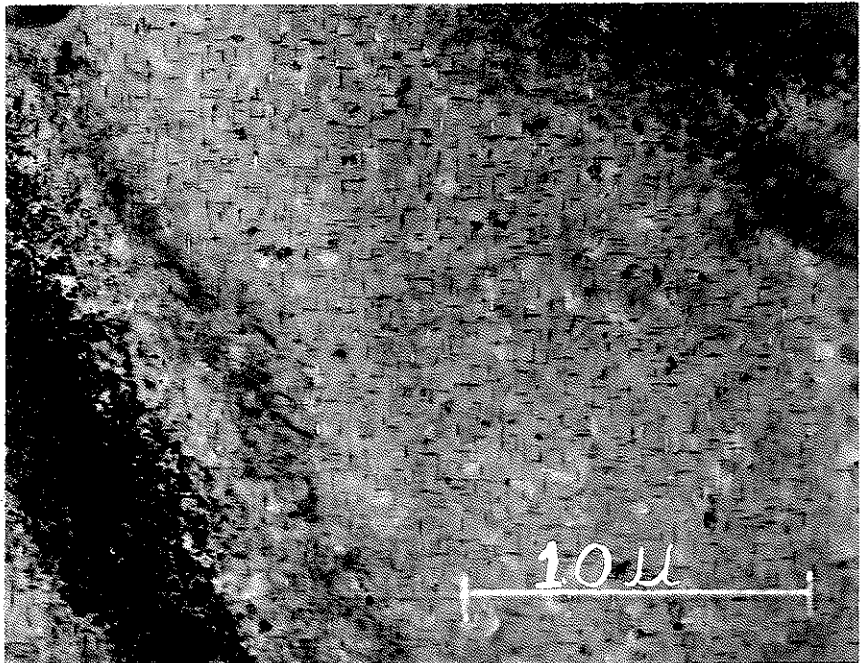
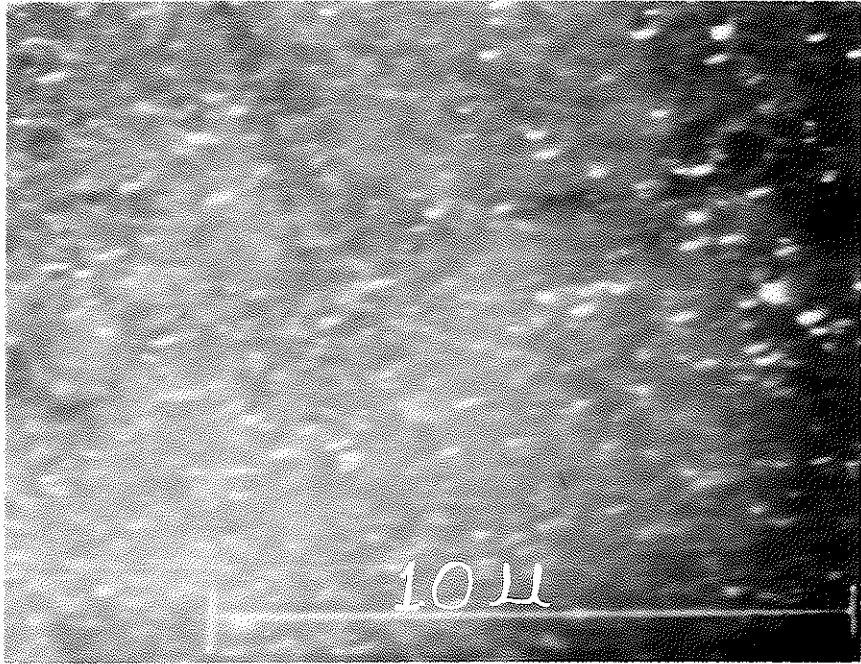


Figure 7:19

Structure of material 30% deformed at 100°C
and aged 188 hours at 190°C. [(001) foil normal]

Figure 7:20

Dark field of Figure 7:19 from (011) precipitate
diffraction spot.

